Fire resistance of LSF wall systems lined with different wallboards including bio-PCM mat

Sayilacksha Gnanachelvam, Anthony Ariyanayagam and Mahen Mahendran

Queensland University of Technology (QUT), Brisbane, Australia

Abstract

Light gauge steel framed (LSF) wall systems made of cold-formed steel studs and lined with different types of wallboards are increasingly used for various purposes. Gypsum plasterboards are commonly used for fire protection purposes, while recently other types of wallboards are being used based on their improved thermal and physical performance but without an understanding of their fire resistance. To increase the thermal mass of LSF wall systems, phase change materials (PCMs) with high thermal storage capacity can be used, but since some organic PCMs increase the fuel load in fire, bio-based PCMs are preferred as they are less flammable than paraffin based PCMs. However, the fire resistance of LSF wall systems incorporated with bio-based PCM has not been investigated. Therefore, this research study investigated the thermal properties of selected wallboards first and then the fire resistance of non-load bearing LSF wall systems lined with different types of wallboards such as gypsum plasterboard, magnesium sulphate board, vermiculux board and fibre cement board using standard fire tests including a thermal mass improved LSF wall system using bio-based PCM mat. Findings revealed that gypsum plasterboard gives the highest fire resistance, whereas the fibre cement board gives the lowest. Importantly, the thermal mass improved LSF wall system did not exhibit any reduction to its fire resistance due to the use of bio-based PCM mat. This paper presents the details of the standard fire tests of LSF wall systems and the results.

Keywords: Phase change materials; Bio-based PCM mat; Gypsum plasterboard; Fibre-cement board; Magnesium sulphate board; Vermiculux board; Thermal properties; LSF walls; Fire tests.

1. Introduction

Light gauge steel framed (LSF) wall systems are widely used as load bearing or non-load bearing elements in the emerging lightweight cold-formed steel (CFS) construction. They are made of CFS studs and lined with different types of wallboards. Thermal mass and fire resistance are two important design parameters for LSF wall systems. Structural failures of steel studs occur in load bearing LSF walls exposed to fire due to the reduction in mechanical properties of CFS at elevated temperatures [1]. Such failures are delayed by the fire protective wallboards, and fire rated gypsum plasterboards are commonly used in LSF walls for this purpose. Many researchers investigated the fire performance of different LSF wall systems lined with gypsum plasterboards [2-4]. Different types of wallboards made of calcium silicate and magnesium oxide are also used as fire protective wallboards [5-8]. Recently, various other types of wallboards are also used in LSF walls due to their improved thermal and physical properties for the purposes of thermal comfort, impact resistance, sound insulation and moisture resistance, for example, magnesium sulphate board, fibre cement board and vermiculux board. However, their fire resistance characteristics have not been adequately investigated. Magnesium sulphate boards are being used to replace magnesium oxide boards because of the lower fire resistance and severe cracking of the latter, caused by higher mass loss at elevated temperatures [7]. However, the fire resistance levels and elevated temperature thermal properties of magnesium sulphate boards are also unknown.

LSF wall systems have lower thermal mass compared to conventional wall systems and thus exhibit poor thermal performance. This affects the indoor thermal comfort level of buildings and creates fluctuations during seasonal variations. Thermal energy storage techniques can be used to avoid indoor temperature fluctuations by increasing the thermal mass of wall systems. Phase change materials (PCMs) with high latent heat storage capacities can be used as thermal energy storage materials in buildings [9]. PCMs absorb or lose considerable energy and undergo a phase transition from solid to liquid or liquid to solid. They melt during daytime and solidify at night times due to the phase transition, and thus help to maintain the indoor thermal comfort level. Commonly, organic micro-encapsulated paraffin PCM is used in building products. However, the organic paraffin PCM, being a flammable material, increases the flammability of these products and affects their fire performance [10-12]. Instead, bio-based PCM materials can be used due to their relatively high ignition resistance and significantly less flammability compared to paraffin-based PCMs [13, 14]. These bio-based PCMs are mostly

made of fatty acid oil esters and are capable of actively performing for thousands of cycles. They are capable of absorbing and releasing a larger amount of heat, similar to other organic paraffin PCMs [13]. Generally, thermal discomfort level is increased in high energy efficient buildings during hot days and heatwave periods. Bio-based PCMs help to reduce thermal discomfort levels with indoor heat stress reduction and improved occupant health [15]. Therefore, bio-based PCM mats are used with gypsum plasterboards to improve the thermal mass of LSF walls. However, their effects on the fire resistance of LSF walls are unknown.

In this study, fire resistance characteristics of commonly used gypsum plasterboard, fibre cement board, vermiculux board and magnesium sulphate boards are investigated when used in LSF wall systems. It initially investigated the elevated temperature thermal properties of magnesium sulphate boards and compared with those of gypsum plasterboards and magnesium oxide boards. Then it investigated the fire performance of LSF wall systems made of all the selected wallboards under standard fire conditions using small-scale fire tests. The insulation based failure times of all the LSF walls were determined and compared to identify the best performing wallboard. Finally the fire performance of a thermal mass improved LSF wall system lined with the best performing wallboard and macro-capsulated bio-based PCM mats was investigated and compared with the commonly used gypsum plasterboard lined LSF walls. This paper presents the details of this study and the results.

2. Materials and chemical compositions

Suitable wallboards are selected based on fire resistance, sound insulation, impact and moisture resistance, durability and economy. Although gypsum plasterboards are commonly used in LSF walls as fire protective wall linings, recently other wallboards such as magnesium oxide board, calcium silicate board and magnesium sulphate board are also used. This section describes the chemical composition of gypsum plasterboard, fibre cement board, magnesium sulphate board, vermiculux board and the bio-based PCM mat.

Gypsum plasterboard core is mainly (>80%) comprised of gypsum (Calcium Sulphate di-hydrate ($CaSO_4.2H_2O$)). Fly ash (<10%), cellulose (<5%), vermiculite (<5%) and a few other additives (quartz, starch and glass fibre) in small percentages are mixed with gypsum to delay the shrinkage cracks, board fall-off and ablation, which increases the fire resistance. Gypsum contains 15-18% of chemically bound water and 4-5% of free water [5]. This water is released as vapour during the dehydration process. The initial density of 16 mm gypsum plasterboard is

13 kg/m^2 and its initial R-value is 0.094 m^{2}K/W. The ambient and elevated temperature thermal properties of the standard gypsum plasterboards are discussed in [16].

Fibre cement board is made of crystalline silica (20-60%), calcium silicate (35-65%), calcium carbonate (30%), calcium aluminium silicate (20%), cellulose (15%) and carbon black (1%). The initial/bulk density of 9 mm thick fibre cement board is 12.5 kg/m^2. Fibre cement boards are used as external wallboards due to moisture resistance, toughness, ductility and crack resistance [17]. They have a lower mass loss at elevated temperatures (22% at 800 °C) [18].

Magnesium sulphate boards are made of magnesium oxide (55%), magnesium sulphate (25%), fibreglass (18%), and filtered wood shavings (2%). Magnesium oxide boards are made of magnesium oxide (MgO) (40-53%), magnesium chloride (MgCl$_2$) (20-35%), perlite, woodchip and fibreglass in different proportions [7]. Magnesium sulphate boards are being used as replacement for magnesium oxide boards, which exhibit lower fire resistance associated with severe cracking caused by higher mass loss at elevated temperatures [7]. A mass loss of about 38 to 57% is reported for different types of magnesium oxide boards [7, 18]. The main difference between the two magnesium boards is the replacement of MgCl$_2$ with MgSO$_4$ in the former, which is considered to eliminate the corrosive action by chloride. The initial density of 10 mm thick magnesium sulphate board is 10.8 kg/m^2 and its R-value is 0.066 m^{2}K/W.

Vermiculux board is a non-combustible board made of calcium silicate (30-60%), vermiculite (30-60%) and some fibres like cellulose (30-60%). Lightweight vermiculux board has a bulk density of 9.6 kg/m^2 and its thickness varies from 20 to 50 mm. Vermiculite is a hydrated laminar material, which expands between 7 and 15 times at elevated temperatures from 700 to 1000 °C [19]. This helps in eliminating severe cracking as it can fill the gaps by expansion.

PCM mat is a flexible mat made of macro-encapsulated bio-based phase change materials in the form of a soft gel at 25 °C, filled within pockets of a poly film (referred to as bio-based PCM mat in this paper). Bio-based PCM mat is mainly comprised of derivatives of fatty acids, fatty alcohols, esters, emulsifiers, thickening agents and proprietary cross linkers. However, the exact percentages of materials are unknown. Organic bio-based PCMs are less flammable compared to the traditional paraffin-based PCMs [13]. Active ingredient weight of 9 mm thick bio-based PCM mat is 2.59 kg/m^2 and the melting point is 23 °C.

3.   Thermal properties

This section describes a series of thermal property tests of magnesium sulphate boards at elevated temperatures to determine their specific heat capacity at constant pressure (c_P), mass loss variations and thermal conductivity. Elevated temperature thermal properties of other boards have been investigated previously and the results are presented in [7, 16]. Simultaneous thermal analyser was used to measure the specific heat capacity at constant pressure (c_P) and mass loss variation according to ASTM E1269-11 [20]. Laser flash apparatus (LFA) was used to measure the thermal diffusivity, which was then used to determine thermal conductivity. Standard procedures to determine the thermal diffusivity using LFA were adopted based on ASTM E1461-13 [21]. The results of elevated temperature thermal properties of magnesium sulphate board are compared with those of magnesium oxide board and gypsum plasterboard.

3.1.   Thermal properties of magnesium sulphate board

Figure 1 shows the variation in specific heat capacity (c_P) of magnesium sulphate board from 25 to 1200 °C at constant pressure. An initial c_P value of 1400 J/kg°C is observed with three peak values. Initially, the specific heat capacity of magnesium sulphate board continues to increase when it is heated and reaches the first and the highest peak value of 6300 J/kg°C at 170 °C. This is due to the dehydration process [22]. Then, a reduction in c_P value is observed and it reaches nearly the base value and remains constant from 270 °C to 360 °C. Twin peak values of 6000 and 5600 J/kg°C are observed at 400 and 460 °C, respectively, with a drop in c_P (4700 J/kg°C) at 430 °C. The specific heat reduces from 600 °C and becomes negative. This means that there is an exothermic energy release due to the decomposition of other elements in this temperature region. Figure 2 shows the mass retention with temperature of magnesium sulphate board, where a total mass loss of 43% (average value) is observed at the final test temperature of 1200 °C. This high mass loss can cause severe cracking at elevated temperatures, leading to premature integrity failures [7]. Thermal conductivity variation of magnesium sulphate board is shown in Figure 3. An initial thermal conductivity of 0.53 W/m°C and a gradual reduction to 0.27 W/m°C at 500 °C with fluctuations are observed. Fluctuations are seen at 150 and 300 °C, which are associated with the peak points in specific heat capacity.
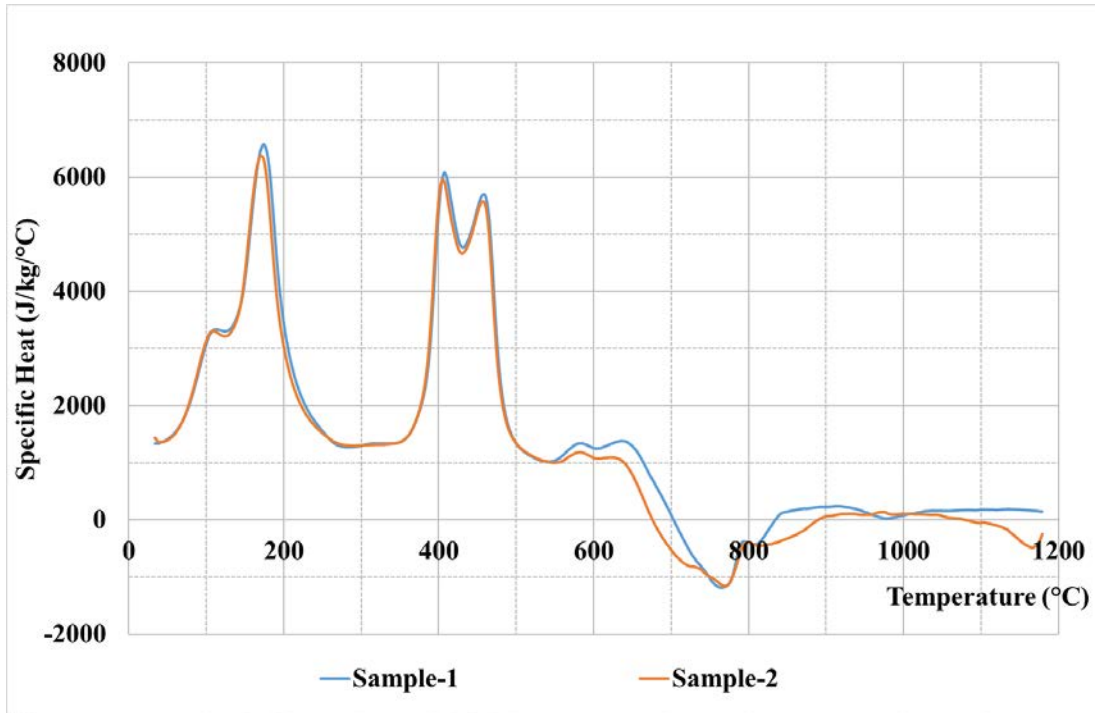
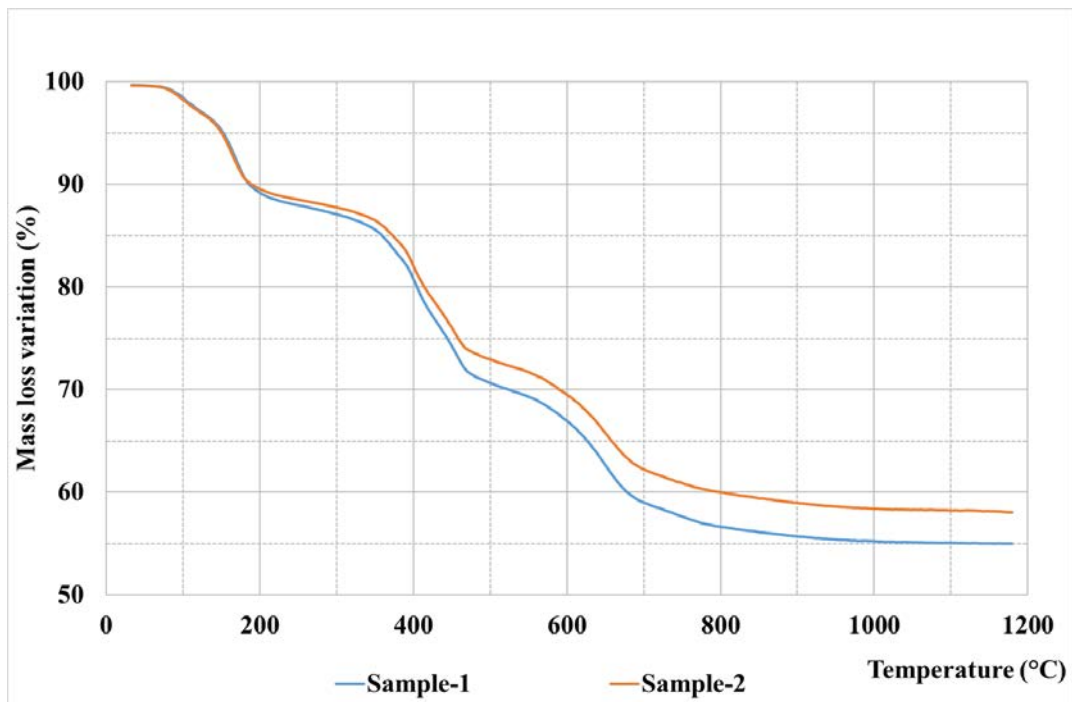Figure 1. Specific heat capacity of magnesium sulphate board

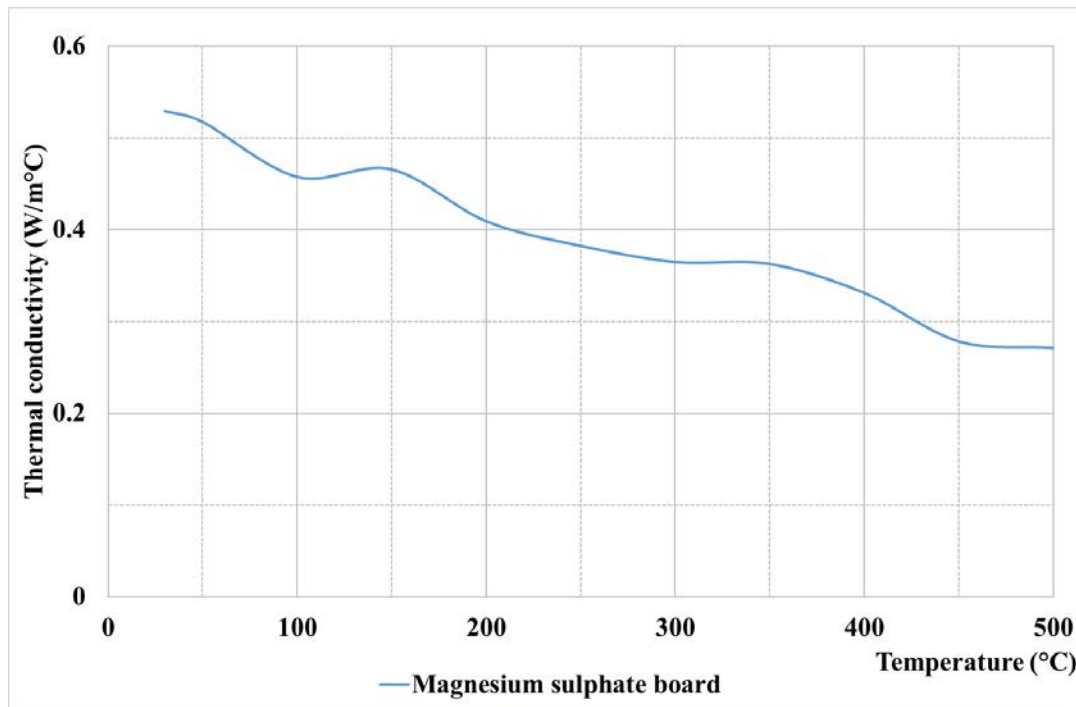Figure 2. Mass loss of magnesium sulphate board

Figure 3. Thermal conductivity of magnesium sulphate board

3.2. *Comparison of the thermal properties of magnesium sulphate board and gypsum plasterboard*

Figure 4 shows the specific heat capacity variations (c_p) of magnesium sulphate board and gypsum plasterboard from 25 to 1200 °C. Their initial c_p values are 1400 and 900 J/kg°C. Two major peaks were observed for magnesium sulphate board, whereas one major peak was observed for gypsum plasterboard. The first major c_p peak at 170 °C for magnesium sulphate board is observed due to dehydration, similar to the major peak in gypsum plasterboard observed around the same temperature (160 °C). Gypsum plasterboard exhibits a higher c_p value of 10,672 J/kg°C, compared to that of 6300 J/kg°C for magnesium sulphate board. Further, two additional peaks observed for magnesium sulphate board around 400 °C are not seen for gypsum plasterboards. This might be due to the additional chemical reactions. These reactions are not discussed here as all the components could not be identified from the material data sheets. These additional peak values observed around 400 °C could be beneficial in fire due to high amount of heat/energy absorption.

Figure 5 compares the mass retention of magnesium sulphate board and gypsum plasterboard with temperature. A total mass loss of 43% is observed for magnesium sulphate board compared to 23% for gypsum plasterboard at the final test temperature of 1200 °C. Elevated temperature thermal conductivity variations of magnesium sulphate board and gypsum

plasterboard are shown in Figure 6. An initial thermal conductivity of 0.53 W/m°C is observed for magnesium sulphate board at 30 °C, whereas it is 0.23 W/m°C for gypsum plasterboard. Gradual reductions in thermal conductivity are observed for both magnesium sulphate board and gypsum plasterboard. The reduced thermal conductivity values at 500 °C are 0.27 and 0.14 W/m°C for magnesium sulphate board and gypsum plasterboard, respectively.
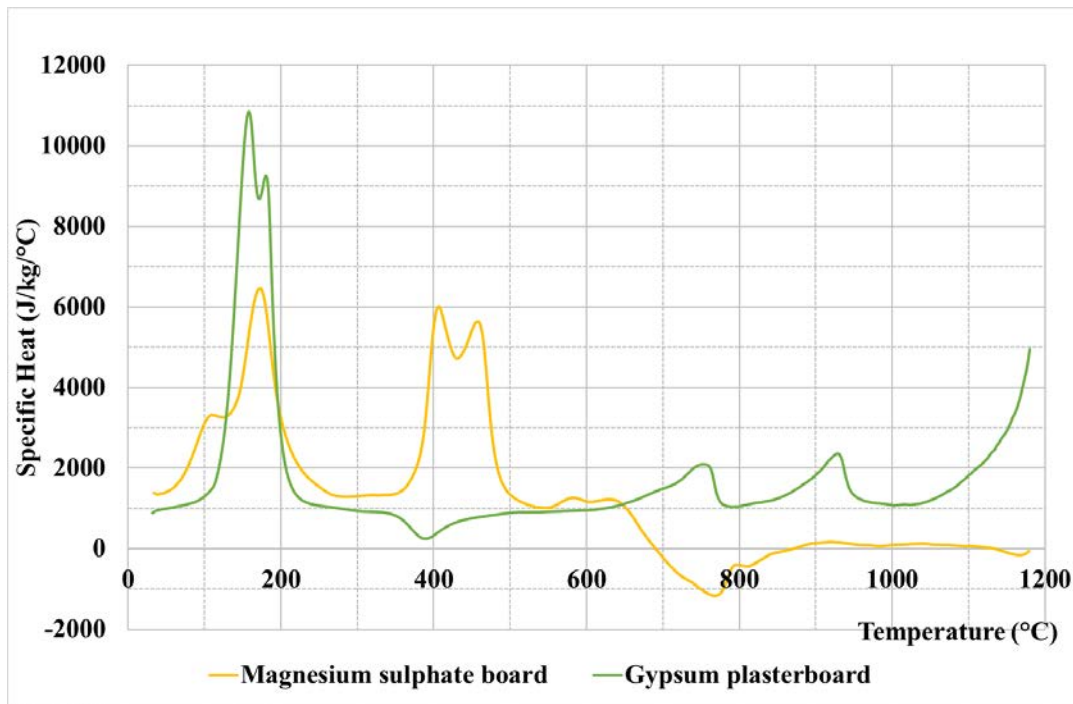

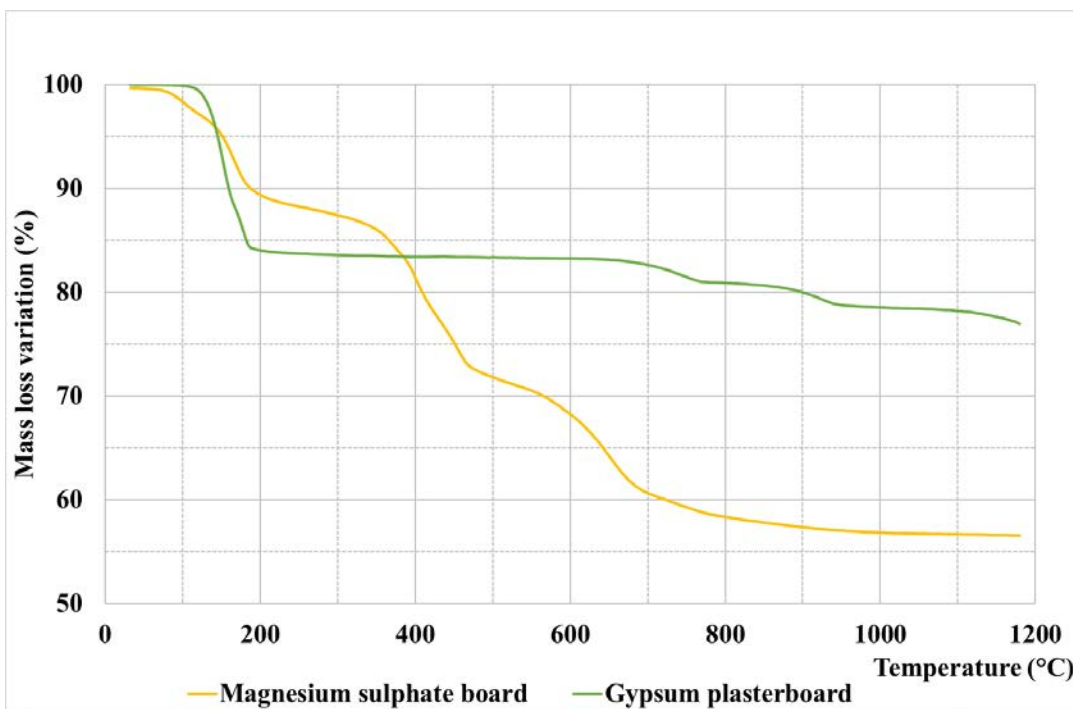Figure 4. Specific heat capacity of magnesium sulphate board and gypsum plasterboard

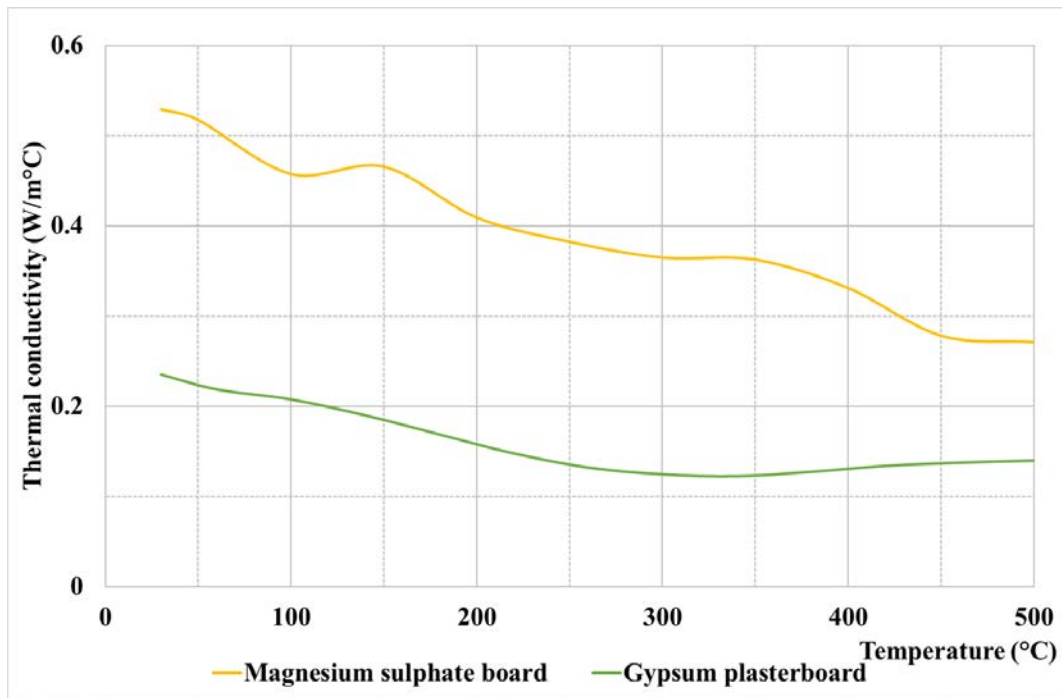Figure 5. Mass loss of magnesium sulphate board and gypsum plasterboard

Figure 6. Thermal conductivity of magnesium sulphate board and gypsum plasterboard

3.3. *Comparison of the thermal properties of magnesium sulphate board and magnesium oxide board*

The measured elevated temperature thermal properties of magnesium sulphate board are compared with those of two different types of magnesium oxide boards reported in Rusthi et al. [7]. Figure 7 compares the specific heat capacity variations (c_p) for magnesium sulphate board and magnesium oxide boards from 25 to 1200 °C. Similar initial c_p values and two major peaks are observed for all three boards. First major twin peaks are observed at 180 and 230 °C in both types of magnesium oxide boards, which were induced by the dehydration process. However, the peak values of Type-1 board are much higher than Type-2 board, and the first major peak of magnesium sulphate board is at 170 °C. The second major twin peaks in all three boards are observed at about 400 and 475 °C. However, these peaks indicate the hydrolysis and pyrolysis reactions in magnesium oxide boards where HCl is released [7].

Figure 8 shows the mass retention of magnesium sulphate board and magnesium oxide board with temperature. Mass losses of 43% and 47% are observed in Type-1 and 2 magnesium oxide boards compared to 43% for magnesium sulphate board at the final test temperature of 1200 °C. Although the chemical composition is different, similar mass loss patterns are observed for all three boards. Elevated temperature thermal conductivity variations for magnesium sulphate board and magnesium oxide boards are shown in Figure 9. Initial thermal conductivity values

are 0.39 and 0.47 W/m°C for Type-1 and Type-2 magnesium oxide boards, compared to 0.52 W/m°C observed for magnesium sulphate board at 50 °C. Thermal conductivity values gradually reduced to half of the initial value at 50 °C for all three boards.
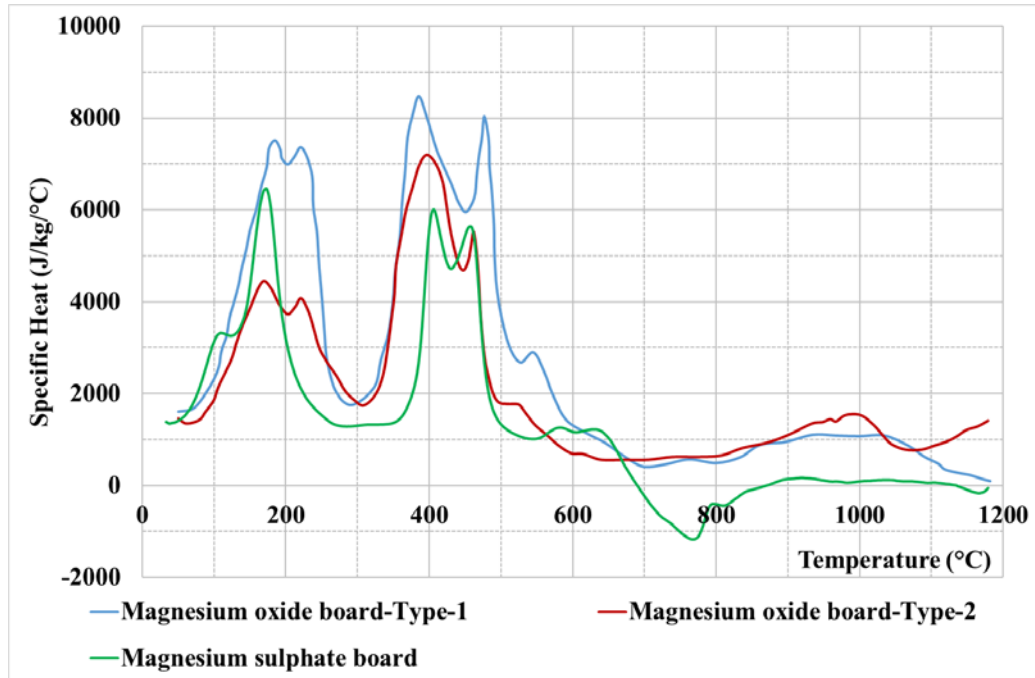

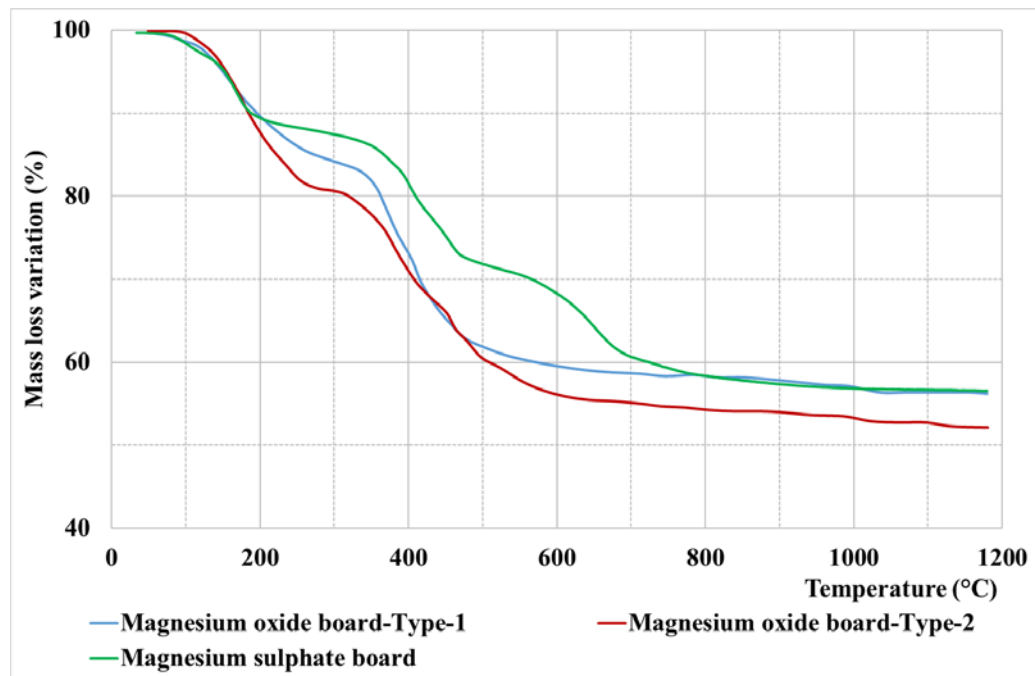Figure 7. Specific heat capacity of magnesium sulphate board and magnesium oxide board

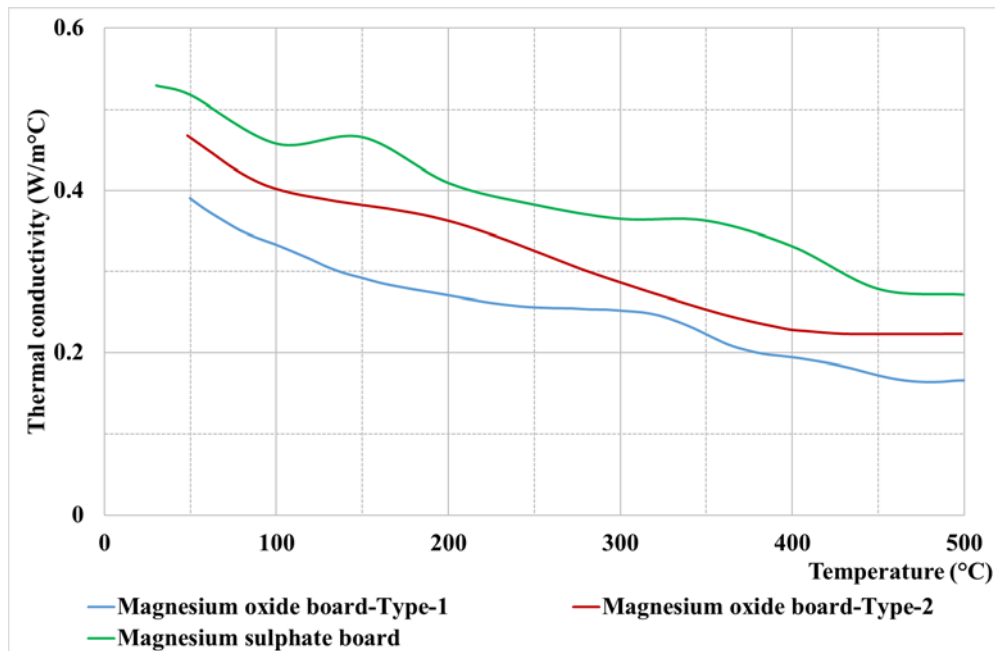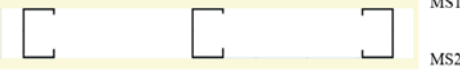Figure 8. Mass loss of magnesium sulphate board and magnesium oxide board

Figure 9. Thermal conductivity of magnesium sulphate board and magnesium oxide board

4. Small-scale fire tests

4.1. LSF wall specimens

Standard fire tests were conducted on five non-load bearing LSF wall systems of 1.4 m width and 1.2 m height based on AS 1530.4 [23]. Fire resistance of load bearing elements is measured under three failure criteria, structural adequacy, integrity and insulation, whereas it is measured under two criteria, integrity and insulation for non-load bearing elements [23]. Structural adequacy is the ability of an element to withstand a load whereas integrity is the ability to resist flames and hot gases from fire side to ambient side in a fire. Insulation failure is based on the ambient side maintaining the temperature below a specified limit, which is 140 °C on average or 180 °C at any point on the surface (maximum) above the room temperature. Table 1 shows the details of the five test specimens used in the fire tests. Test specimens 1 to 4 were lined on both sides with single layer of 16 mm gypsum plasterboard, 9 mm fibre cement board, 10 mm magnesium sulphate board and 20 mm vermiculux board, respectively. Test specimen 5 was lined on both sides with a combination of a bio-based PCM mat with a layer of 16 mm gypsum plasterboard. Figure 10 shows the stud arrangement used in LSF walls, made of 0.95 mm thick tracks and 0.75 mm thick studs made of G550 steel (minimum yield strength of 550 MPa). The dimensions of studs and tracks were 90×36×7×0.75 mm and 92×40×0.95 mm, respectively. Studs were located inside the tracks at 450 mm spacing and fastened with 16 mm long D-type flat head self-drilling screws. Wallboards were screw fastened only to studs.

Table 1. Test wall configurations

Test	Wall configuration	Description
1	PB1 / PB2	Single layer gypsum plasterboard (SLPB)
2	FC1 / FC2	Single layer fibre cement board (SLFC)
3	MS1 / MS2	Single layer magnesium sulphate board (SLMS)
4	VC1 / VC2	Single layer vermiculux board (SLVC)
5	PB1 BP1 / BP2 PB2	Single layer gypsum plasterboard (SLPB) and bio-based PCM (BP) mat inside
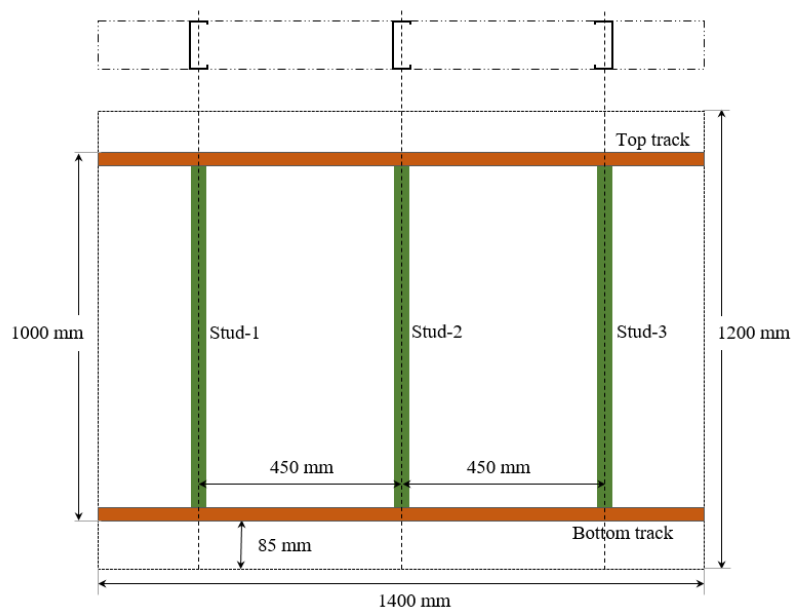
Figure 10. Stud and track arrangements

4.2. Test specimen fabrication and test method

4.2.1. Test specimen fabrication

Test specimens 1 to 4 were all lined with single layer of wallboard on both sides (Table 1). Each board layer consisted of three pieces, 1200×1200 mm, 1200×100 mm and 1200×100 mm. The 1200×1200 mm board was placed in the centre and fastened to all three studs. The two small boards (1200×100 mm) were placed on the right and left sides of the larger board and

connected to both top and bottom tracks. This increased the wall panel width to 1400 mm and allowed the specimen to be fixed to the furnace. D-type self-drilling countersunk screws of 36 mm length were used to fasten the boards at 300 mm spacing along the studs. Thermocouples were attached to the stud and board surfaces. The joints on the board layer were filled with two layers of plaster joint filler compound with sealing paper tape placed between them.

Test specimen 5 was lined with a 16 mm thick layer of gypsum plasterboard placed outside and a bio-based PCM mat placed inside. The same fabrication details used for the other specimens were used. However, the bio-based PCM layer of 1000×1000 mm was placed in the centre to cover the fire exposed area of the furnace. Further, the holes for the thermocouples were made in a pattern so that they did not make any leakages on the PCM pockets.

4.2.2. *Test set-up and thermocouple arrangements*

For Test specimens 1 to 4, 24 K-type thermocouple wires were attached throughout the cross-section at various locations, ie. five on fireside, four on fireside cavity, three on stud hot flange, three on stud cold flange, four on ambient side cavity and five on ambient side. Similarly, 34 K-type thermocouple wires were attached to Test specimen 5. In addition, five thermocouple wires were located between the fire side plasterboard and bio-based PCM mat and another five thermocouple wires were located between bio-based PCM mat and ambient side plasterboard. Figure 11 shows the thermocouple arrangements. Thermocouples were placed on each surface at top left (T-L), top right (T-R), centre (C), bottom left (B-L) and bottom right (B-R). The small holes made on wallboards for thermocouple wires were sealed with plaster filler compound. Small-scale standard fire tests were conducted using a gas furnace with thermocouple wires connected to a data logger to record the fire test data (Figure 12). The external gas supply to the furnace was terminated, when any of the ambient side thermocouples recorded a temperature exceeding the average or maximum insulation failure temperature.
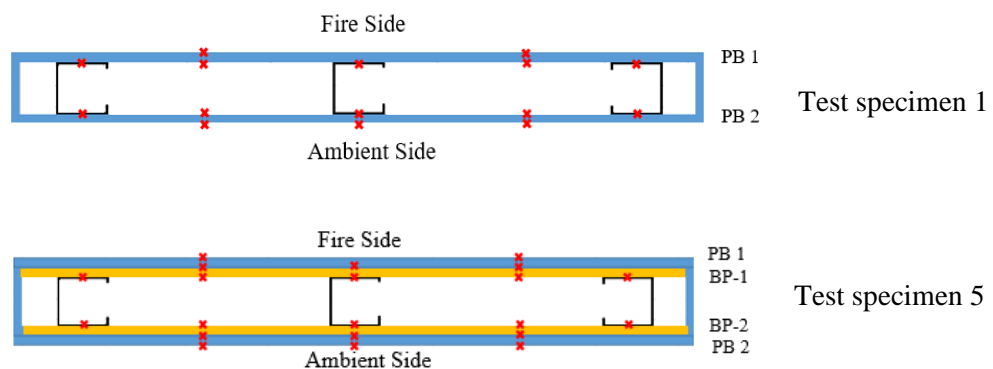

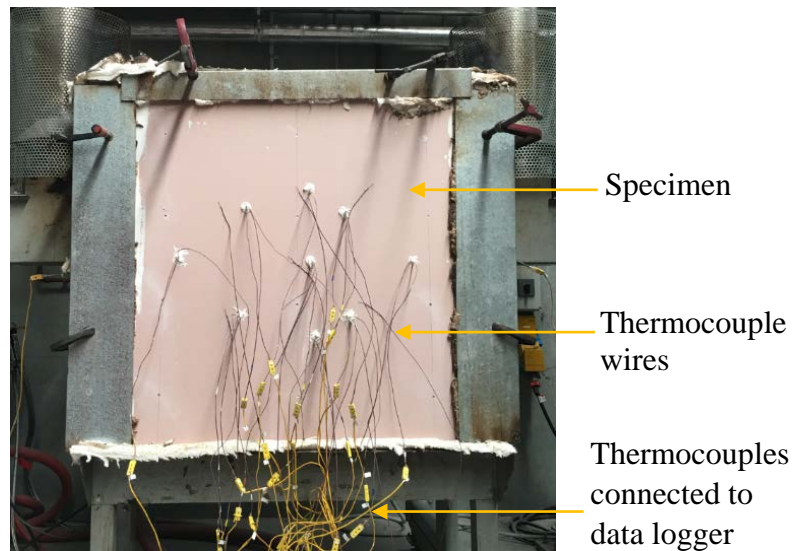
Figure 11. Thermocouple arrangements

Figure 12. Fire test set-up

4.3. Test observations

4.3.1. Test 1 (SLPB)

Figure 13 (a) and (b) show the observations from Test 1 for LSF wall system lined with single layer of gypsum plasterboard on both sides. Smoke was seen at 30 s, reduced after 5 min and was visible again at 7 and 25 min. Smoke was due to the burning of paper on both sides of the plasterboards. Water drops were visible on the top of the furnace and on the floor below the furnace after 11 min and again from 28 to 48 min. Dripping of water was caused by the dehydration of gypsum plasterboard. Discolouration of ambient side plasterboard surface commenced at 84 min and the board fully turned dark at around 133 min. The test was stopped at 143 min, when the average temperature of the ambient side was nearly 200 °C.

Figure 13 (b) shows the specimen after being removed from the furnace. The first layer of plasterboard on the fireside (PB1) had fully burnt and fell-off from the panel. The paper surface of the gypsum plasterboard connected to stud on the ambient side (PB2) had turned into grey. No cracks were visible on the unexposed side of the ambient side plasterboard (PB2), but cracks were seen on its exposed side.

(a) Discolouration of ambient side plasterboard   (b) Plasterboard and stud after the test

Figure 13. Observations from Test 1

4.3.2.   Test 2 (SLFC)

Figure 14 (a) and (b) show the observations from Test 2 for LSF wall lined with single layer of fibre cement board. Smoke was visible after 2 min at the top and bottom of the specimen. Discolouration of the ambient side fibre cement board (FC2) started at the top left corner at 3 min and continued. It was also seen at the right bottom corner of FC2 after 9 min. Excessive smoke was observed after 9 min. Cracks started to appear on FC2 after 14 min, where minor cracks were visible on the left side middle and bottom at 14 and 15 min, respectively (Figure 14 (a)). One major crack appeared on the left side top at 24 min, where discolouration was seen. Another major crevasse was seen on the right side of the board along the vertical joints at 25 min as shown in Figure 14 (b). The flame was visible through the crevasse along the joint at 26 min, where the ambient side temperature reached 205 °C. The test was stopped at 31 min. Significant colour changes and cracks were seen on the ambient side of fibre cement board after the test. However, no water droplets were observed during this period.

(a) Cracking and discolouration   (b) Major crack through vertical joint

Figure 14. Observations from Test 2

4.3.3. Test 3 (SLMS)

Figure 15 shows the observations from Test 3 for LSF wall lined with single layer of magnesium sulphate board. Initially, discolouration was visible on the top left corner after 4 min. Smoke was seen after 6 min and a burning smell was sensed at around 8 min. Ambient side magnesium sulphate board (MS2) started to darken at 11 min. Cracks were seen after 13 min, where the initial crack appeared on the top left corner, the discolouration started and another crack was seen at the bottom left at 15 min. A strong burning smell was noticed again at around 23 min. The ambient side of MS2 started to darken at 24 min. Cracks appeared again at 33 min on the top left and right boards near the screws, which connected the studs and the board. Further cracks were seen on the middle of the board and along the screw attached to the centre of the panel at 37 min. Smoke started to escape through major cracks at 38 min. Discolouration of the ambient side was observed at 43 min and the test was terminated at 45 min when the ambient side temperature reached the maximum insulation failure temperature (204 °C). Figure 15 (b) shows the fireside surface of the specimen after being removed from the furnace. The fire side board surface was burnt and discoloured into light grey, with severe cracking. Most of the cracks were seen at the screw locations/attachments. This might be due to the higher mass loss and the restraint due to screw connections.
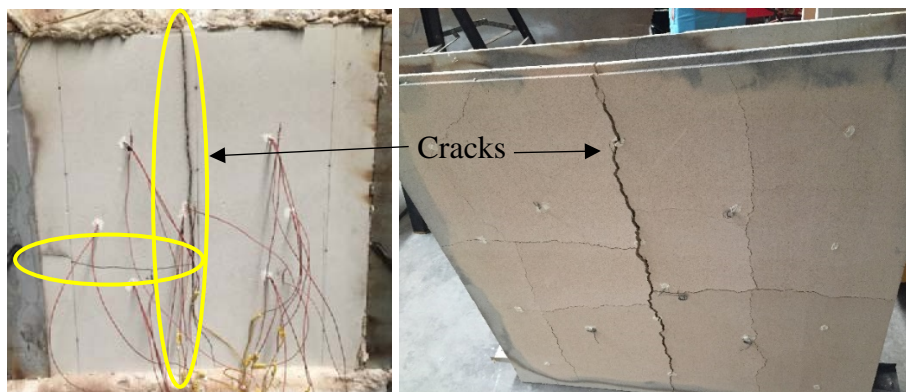
(a) Cracking and discolouration
of ambient side board

(b) Fire side of the specimen
after the test

Figure 15. Observations from Test 3

4.3.4. Test 4 (SLVC)

Figure 16 shows the observations from Test 4 for the LSF wall lined with single layer of vermiculux board. Initially, smoke was visible from the top left after 4 min. Discolouration on the ambient side vermiculux board (VC2) started at 18 min. Small cracks started to appear on the left side middle after 28 min. The crack appeared vertically at the centre at 32 min. Further, the vertical crack extended throughout the length at the centre after 34 min. Discolouration started to occur around the left side crack after 37 min, and also the crack extended towards the centre with the increment in the gap/crack thickness. The board cracked in half through the middle at 38 min, however, the test was continued, and the maximum insulation failure temperature was reached (200 °C) at 47 min. The test was stopped at 53 min. Figure 16 (b) shows the fire side surface of the specimen after the test. Vermiculux board was burnt on the fire side and discoloured into a dark shade of greyish beige, with severe cracking.

(a) Cracking and discolouration
of ambient side board

(b) Fire side of the specimen
after the test

Figure 16. Observation from Test 4

4.3.5. Test 5 (SLPB-BP)

Figure 17 shows the observations from Test 5 for the LSF wall lined with a combination of gypsum plasterboard layer and bio-based PCM mat. Smoke caused by paper burning was seen after 1 min, but reduced at 10 min. It started again at 25 min and continued throughout the test. This is due to the burning of the paper on the board surfaces and the evaporated PCM from the board. Dripping of PCM was initially seen on the floor from the right side bottom corner of the test specimen at 26 min. Initial dripping was a thick white liquid droplet and later the colour turned to light greenish grey/sage after the dripping volume increased. Dripping of PCM rate increased at 31 min with an increment in grey smoke. The average temperature of the molten PCM on the floor was around 330 °C. Thick white liquid drops were seen on the floor below the left corner of the specimen at 40 min, which might be due to the melting of poly film. However, the spill stopped within a minute at the left-hand corner. Spill continued on the right bottom corner until 50 min and then the flow rate reduced. Again, the spill was increased at 55 min and the smoke also increased at 60 min. This might be due to the melting of the second PCM layer, which was on the ambient side. A spill of the creamy textured liquid stopped at 75 min. Water drops were visible on the plasterboard surface at 66 min. This might be due to the dehydration of the ambient side plasterboard. Further, water drops were seen on the floor below the furnace at 71 min (no creaminess or dark colours and drops dried after some time).

Discolouration started on the ambient side gypsum plasterboard at 87 min. The test was terminated at 115 min when the maximum insulation failure temperature was reached. A flame was seen at 116 min on the right-side bottom corner of the specimen, where the molten PCM leaked. The flame was observed through the exhaust after 122 min. Significant colour change (light brown to dark brown) was seen on the ambient side plasterboard, which stayed brisk with no cracks. The gypsum plasterboard (PB1) on the fire side fully burnt and fell-off from the panel, while the surface of gypsum plasterboard on the ambient side (PB2) exposed to fire was fully burnt and discoloured into grey. Although cracks were visible on PB2, it retained its geometry without falling-off. Bio-based PCM mats placed on both fire and ambient sides had melted during the fire test. The colour of the fire side gypsum plasterboard fall-off in this test (Figure 17 (b)) had slightly changed/darkened compared to the fire side gypsum plasterboard fall-off in Test 1 (Figure 13 (b)). This might have occurred due to the melting of PCM.

(a) Smoke and melted PCM leakage   (b) Discolouration and fall-off on
                                        the fire side after the test

Figure 17. Observations from Test 5
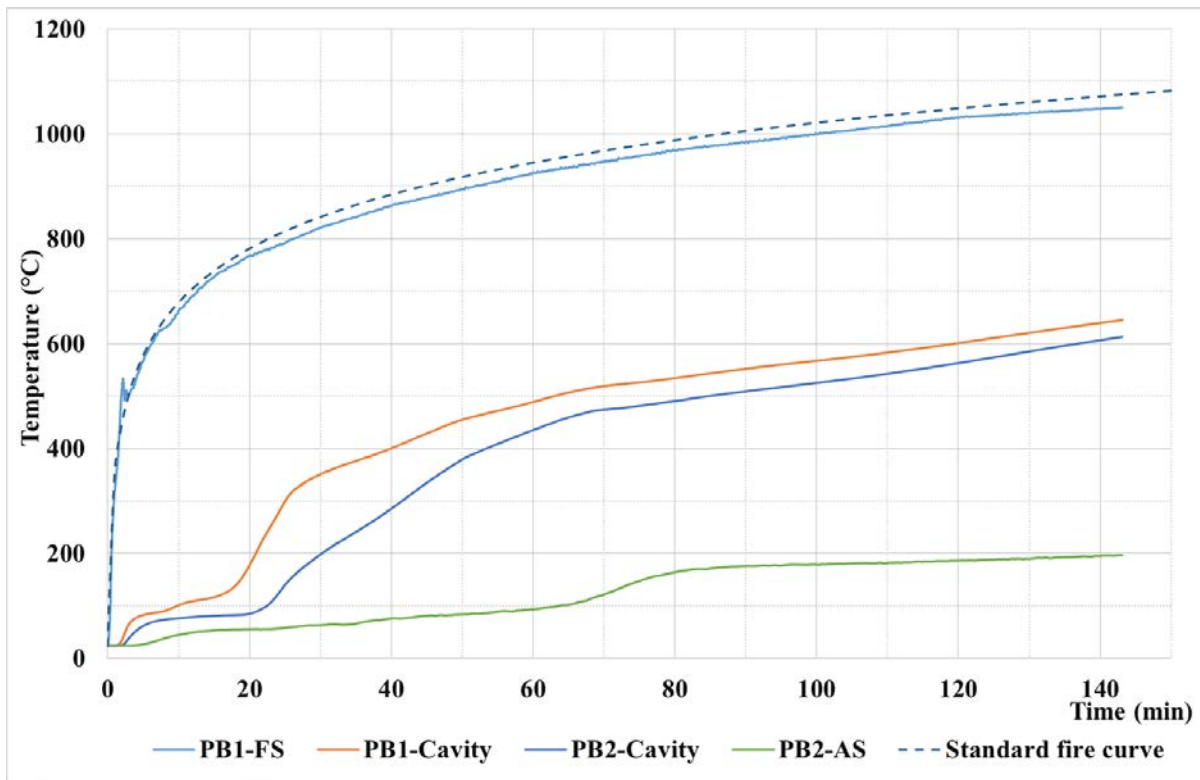
5.   Test Results

5.1. Test 1 (SLPB)

Figure 18 (a) shows the average time-temperature profiles measured on the wallboards of Test specimen 1 lined with single layer of gypsum plasterboard. Fire side temperature of the test had a maximum deviation of 20 °C from the standard fire curve, which is below the acceptable limit specified in AS 1530.4 [23]. Initially, the temperatures of all plasterboard layers were maintained at a constant value less than 100 °C for a certain period of time, which is due to the dehydration effects. Time taken to reach 100 °C was 10, 22 and 65 min for PB1-Cavity, PB2-Cavity, and PB2-AS, respectively. This is similar to the observations of Ariyanayagam and Mahendran [5]. Sudden increments were observed in the plasterboard temperatures after the dehydration process. Further, the temperature gradient for PB1-Cavity and PB2-Cavity reduced after 60 min and continued to have a constant difference until the end.
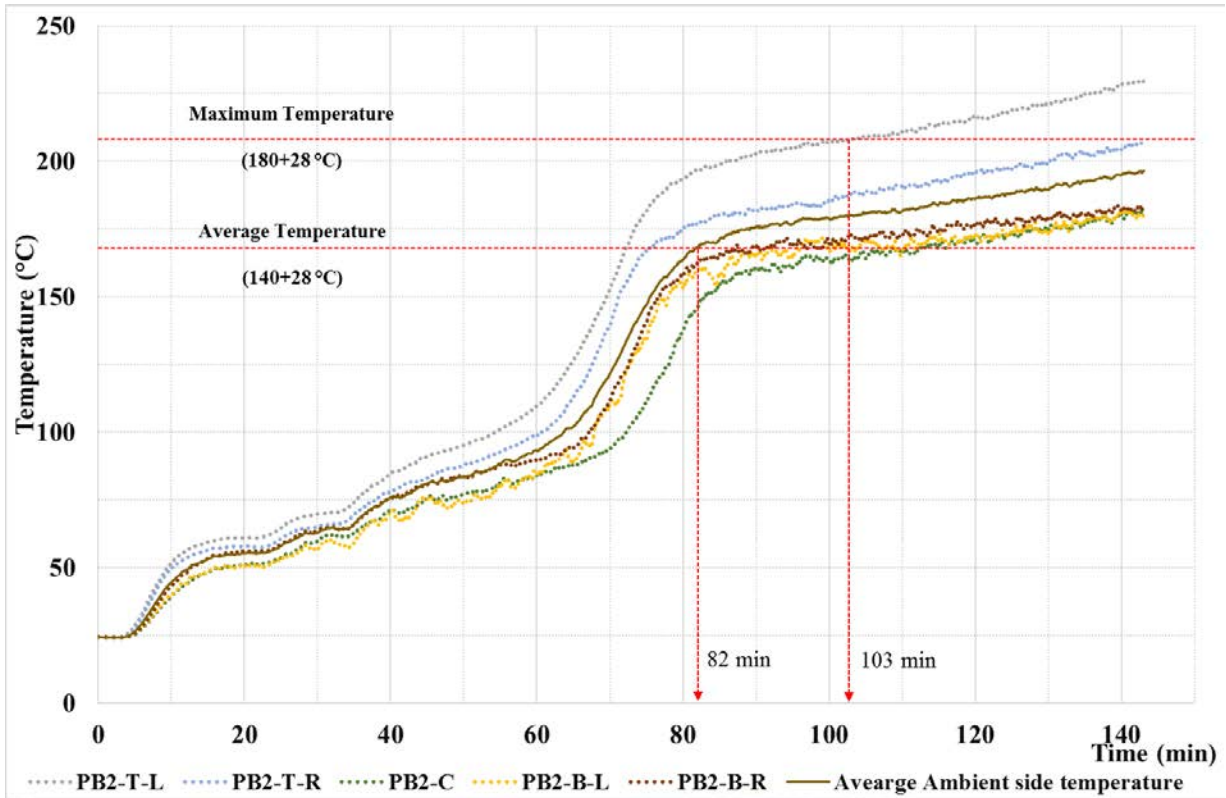
Figure 18 (b) shows the measured individual thermocouple readings and the average temperatures for the ambient side plasterboard (PB2). Average insulation failure temperature limit of 168 °C was observed at 82 min (initial temperature was 28 °C) whereas the maximum insulation failure temperature limit of 208 °C was observed after 103 min. However, the test was continued until 143 min.

Figure 18 (c) shows the average time-temperature profiles of stud hot flange (HF) and cold flange (CF). The maximum HF temperature of 650 °C was reached at 143 min. The maximum

difference of 160 °C between the HF and CF temperatures was seen at 40 min. The HF temperature is a prime factor affecting the structural adequacy of load bearing LSF walls. The HF temperature was 400 °C at 36 min with the corresponding CF temperature of 250 °C. Therefore, based on the limiting HF temperatures for respective load ratios (LR) [24], the structural adequacy based fire resistance time of 36 min can be achieved for a LR of 0.5. This simple approach was used in this study to determine the structural failure times approximately for comparison purposes.

(a) Average gypsum plasterboard temperatures

(b) Ambient side gypsum plasterboard (PB2) temperatures
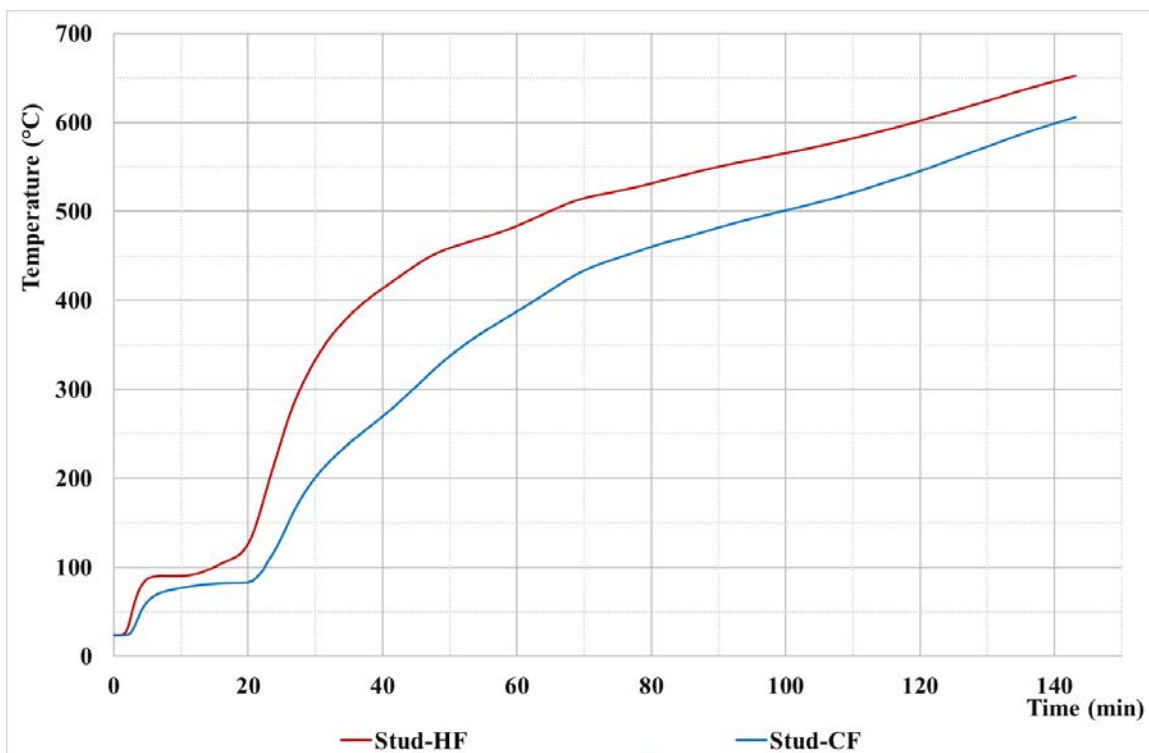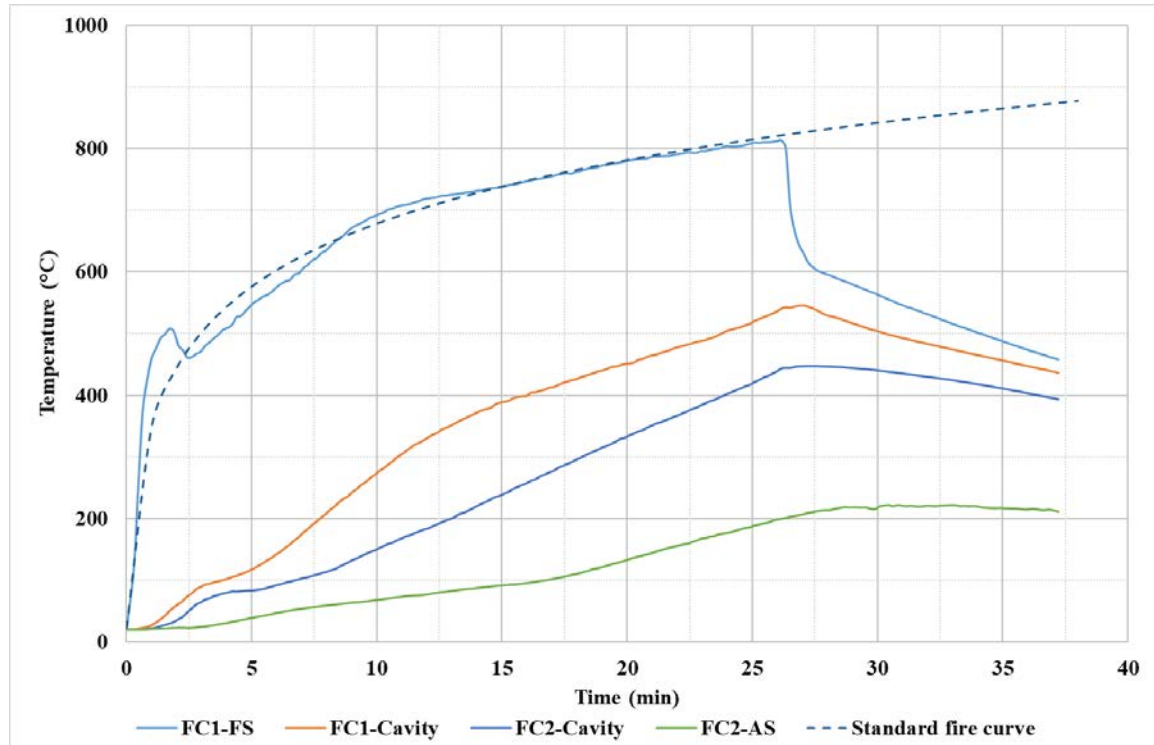

(c) Average stud HF and CF temperatures

Figure 18. Fire test results of Test specimen 1
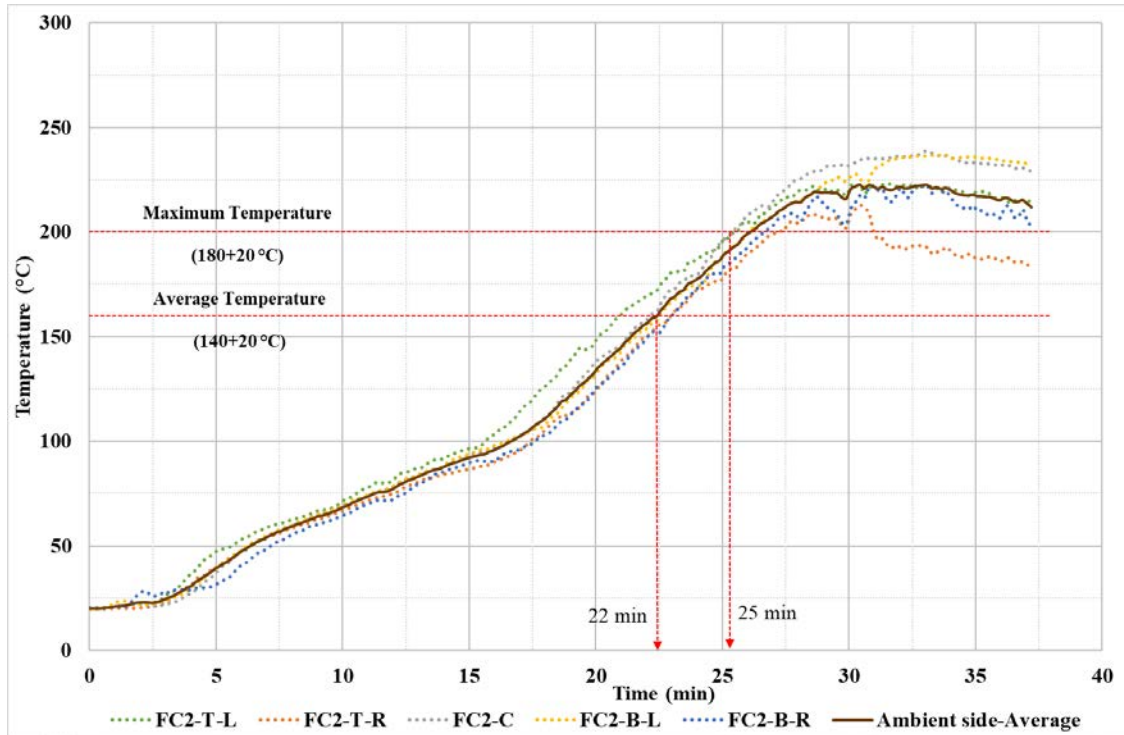
5.2. Test 2 (SLFC)

Figure 19 (a) shows the average time-temperature profiles measured on the wallboards of Test specimen 2 lined with single layer of fibre cement board. Fire side temperature of the test agreed well with the standard fire curve with small fluctuations. No temperature plateaus are observed in this test. Temperature profiles exhibit continuous increment throughout the test.

Figure 19 (b) shows the measured individual thermocouple readings and the average temperatures on the ambient side fibre cement board (FC2). The average insulation failure temperature limit of 160 °C was reached at 22 min (initial temperature was 20 °C), whereas the maximum insulation failure temperature limit of 200 °C was reached at 25 min. However, the test was continued until 27 min.

Figure 19 (c) shows the average time-temperature profiles of stud HF and CF. The maximum HF temperature was 530 °C at 27 min while the maximum difference between HF and CF temperatures was 160 °C at 20 min. At 16 min, the HF temperature reached 400 °C while the CF temperature was 240 °C. Hence a structural adequacy based fire resistance time of 16 min can be achieved for a LR of 0.5 [25].

(a) Average fibre cement board temperatures

(b) Ambient side fibre cement board (FC2) temperatures
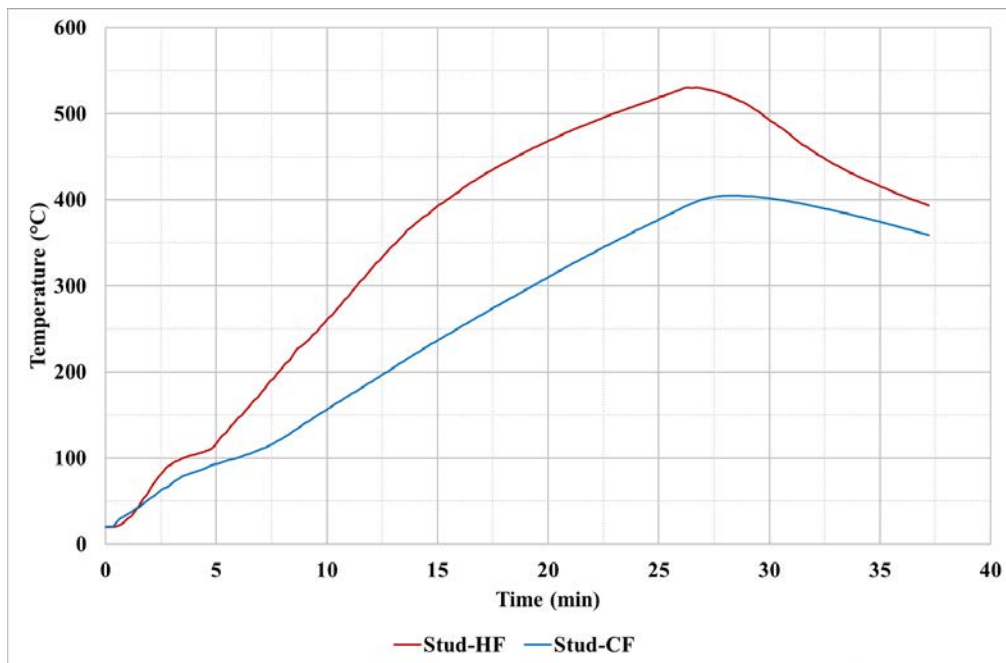
(c) Average stud HF and CF temperatures

Figure 19. Fire test results of Test specimen 2
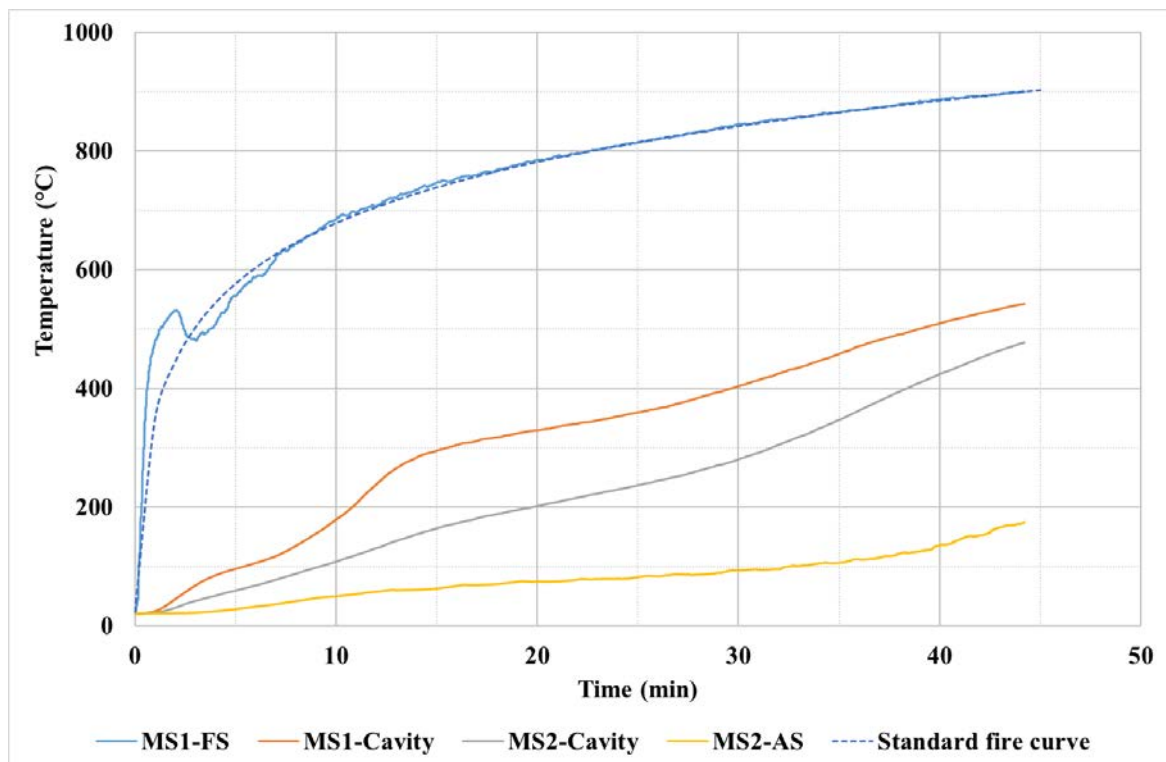
5.3. Test 3 (SLMS)

Figure 20 (a) shows the average time-temperature profiles measured on the wallboards of Test specimen 3 lined with single layer of magnesium sulphate board. Fire side temperature agreed
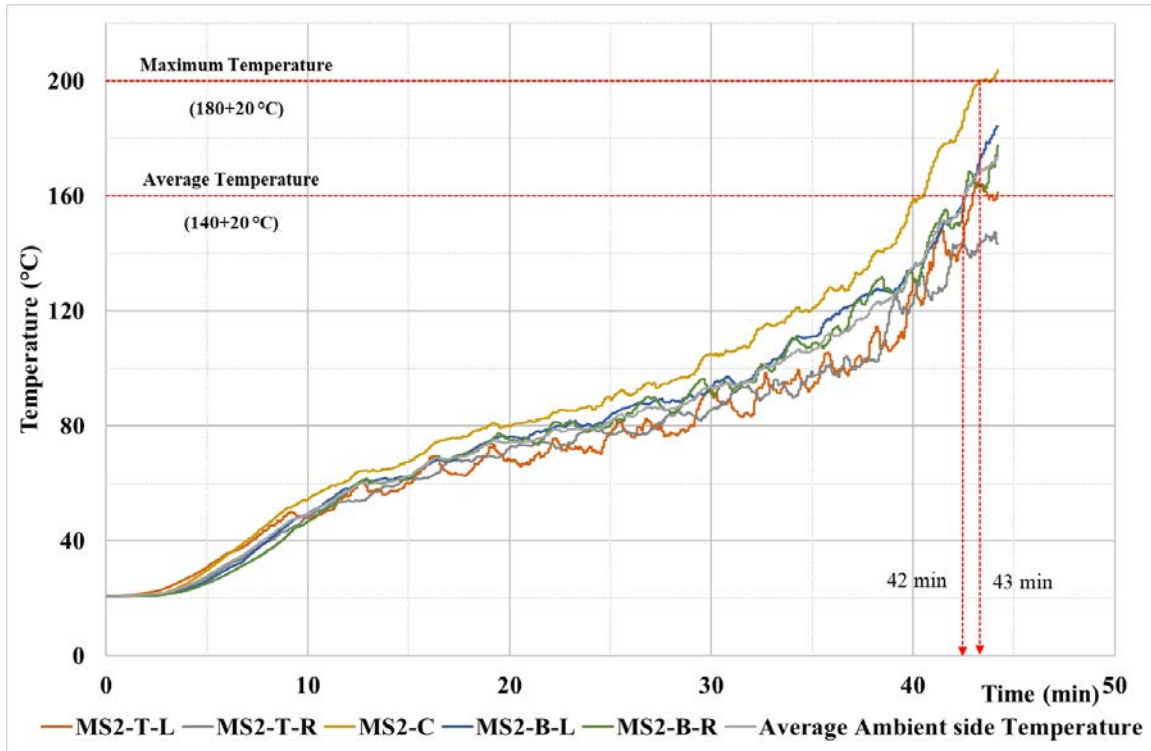
well with the standard fire curve within the limit in [23]. Temperatures of all surfaces showed continuous increment throughout the test and no temperature plateaus were observed.

Figure 20 (b) shows the measured individual thermocouple readings and the average temperatures on the ambient side magnesium sulphate board (MS2). Average insulation failure temperature limit of 160 °C was reached at 42 min (initial temperature was 20 °C), while the maximum insulation failure temperature limit of 200 °C was reached at 43 min, and the test was terminated at 44 min.

Figure 20 (c) shows the average time-temperature profiles of stud HF and CF. The maximum HF temperature was 550 °C at 44 min while the maximum difference between HF and CF temperatures was 160 °C at 31 min. The HF temperature was 400 °C at 30 min with the CF temperature of 250 °C. Hence the structural adequacy based fire resistance time can be estimated as 30 min based on the limiting HF temperature for a load ratio of 0.5 [24].

(a) Average magnesium sulphate board temperatures

(b) Ambient side magnesium sulphate board (MS2) temperatures
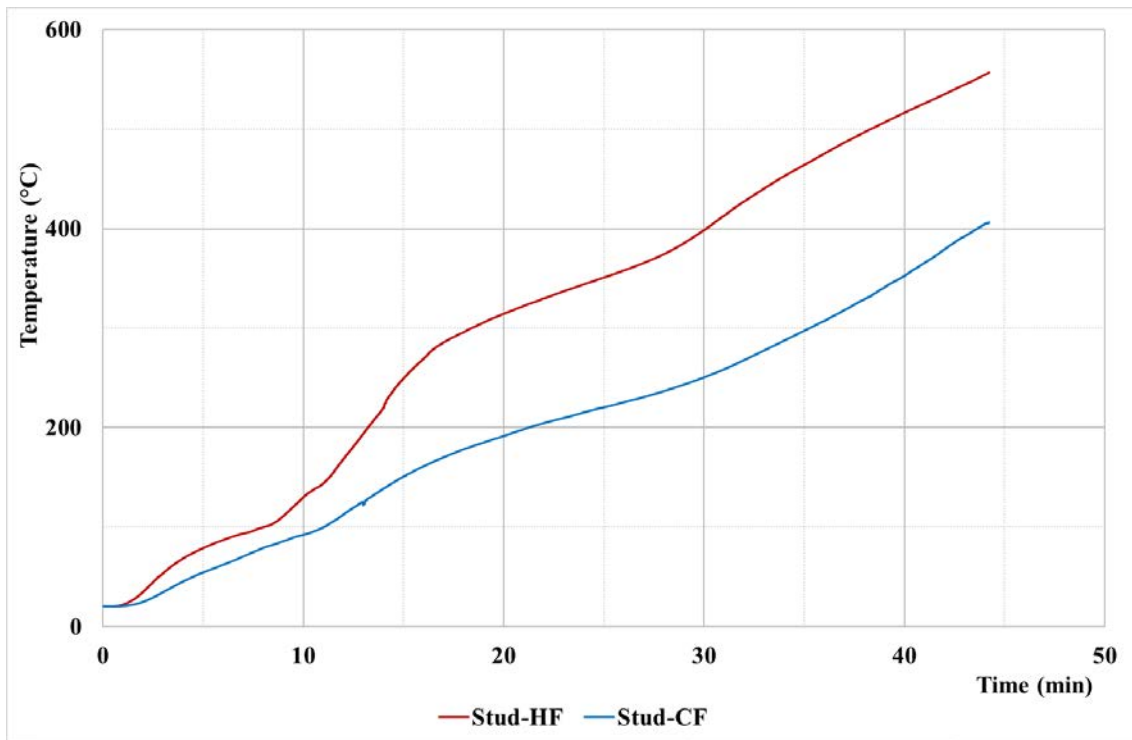
(c) Average stud HF and CF temperatures

Figure 20. Fire test results of Test specimen 3

5.4. Test 4 (SLVC)

Figure 21 (a) shows the average time-temperature profiles measured on the wallboards of Test specimen 4 lined with single layer of vermiculux board. Although the fire side temperature exceeded the standard fire curve, it was within the limit given in [23]. Temperatures of all surfaces show continuous increment throughout the test.

Figure 21 (b) shows the measured individual thermocouple readings and the average temperatures on the ambient side. Both average and maximum insulation failure temperature limits of 160 and 200 °C were reached at 47 min (initial temperature was 20 °C). Figure 21 (c) shows the average stud HF and CF time-temperature profiles. The maximum HF temperature of 650 °C was reached at 53 min while the maximum temperature difference between HF and CF of 120 °C was seen from 20 to 40 min. The critical HF temperature of 400 °C for a load ratio of 0.5 [25] was reached at 24 min with the corresponding CF temperature of 260 °C, giving the structural adequacy based fire resistance time of 24 min.
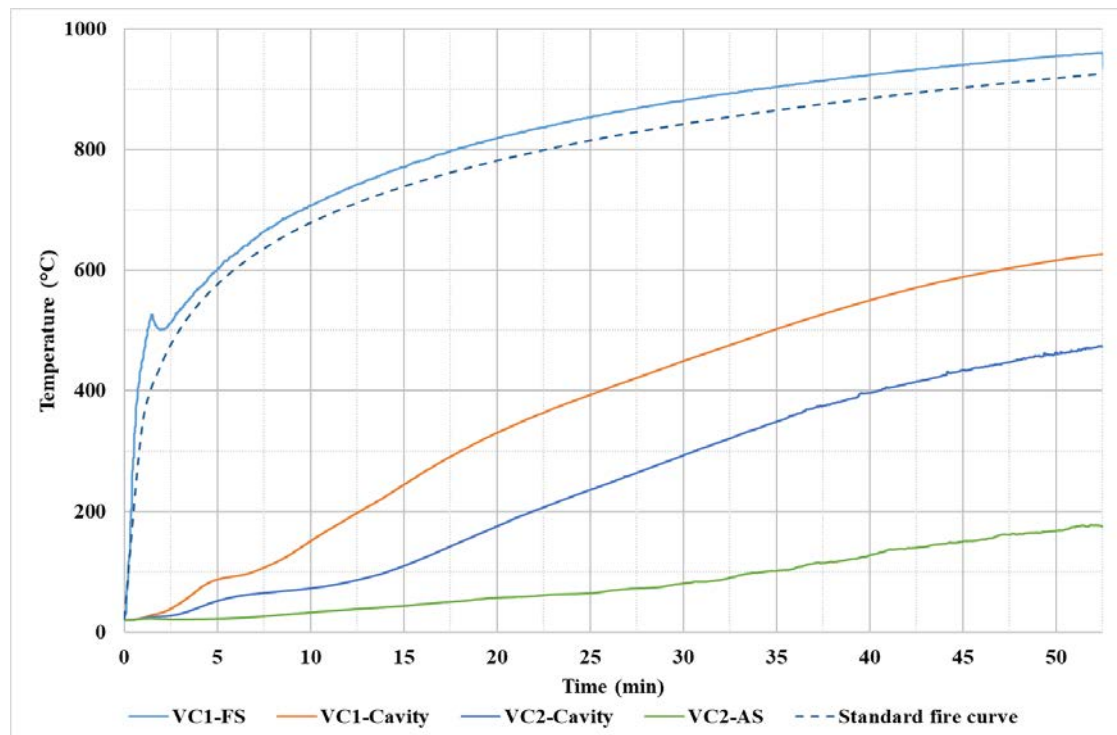
(a) Average vermiculux board temperatures

(b) Ambient side vermiculux board (VC2) temperatures
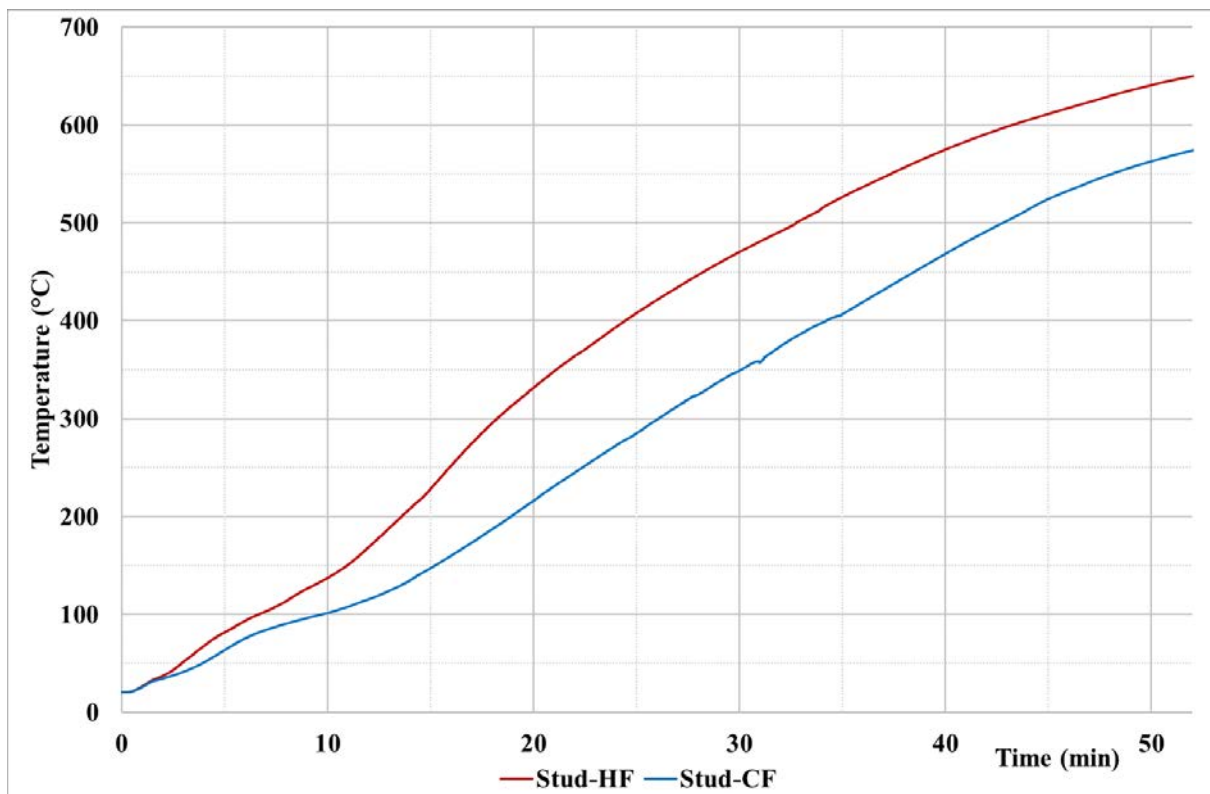
(c) Average stud HF and CF temperatures

Figure 21. Fire test results of Test specimen 4

5.5. Test 5 (SLPB-BP)

Due to the superior performance of gypsum plasterboard observed in the last four tests, this test used gypsum plasterboard lining and bio-based PCM mat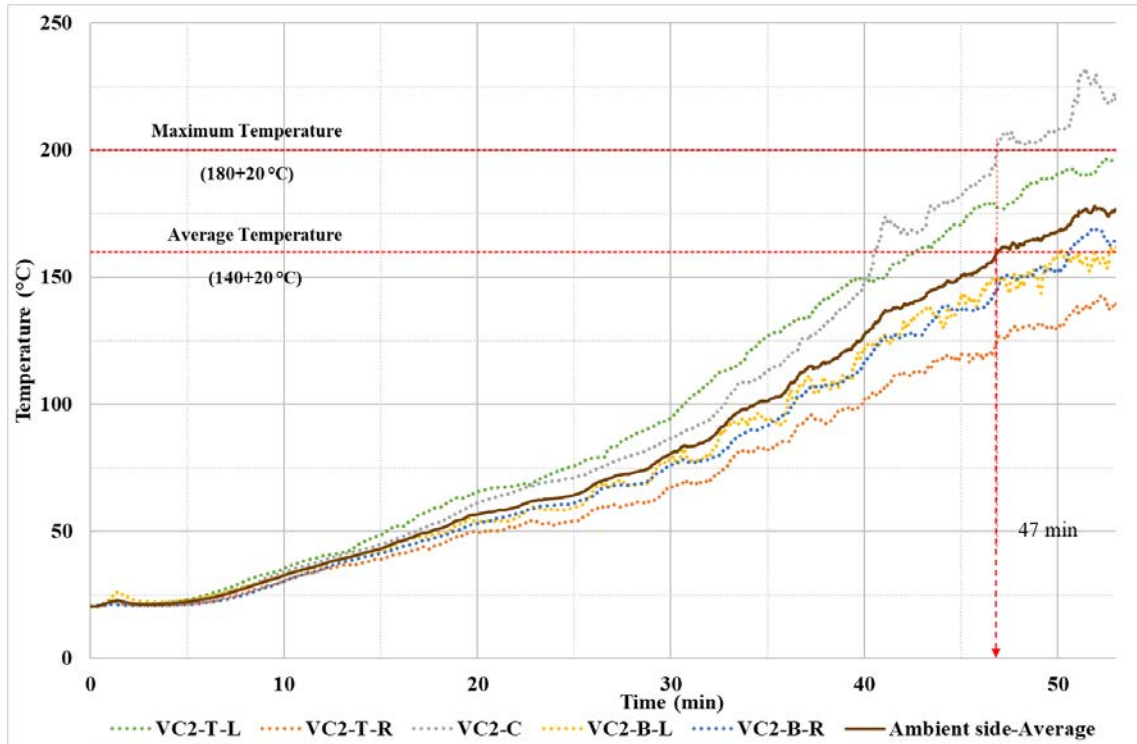. Figure 22 (a) shows the average time-temperature profiles measured on the wallboards of Test specimen 5 lined with single layer of gypsum plasterboard on the exterior and bio-based PCM mat placed on the interior. Fire side temperatures agreed well with the standard fire curve and were within the limit given in [23]. Initially, the temperatures of all gypsum plasterboard surfaces and the bio-based PCM mat surfaces were maintained at a constant value, less than 100 °C for a certain period of time due to the dehydration process and the heat absorption capacity of the PCM. Sudden increments with fluctuations are observed in the temperature on both sides of the bio-based PCM mats on fire and ambient sides. This might be due to the melting of PCM. Further, the gradients of the temperature of surfaces (BP-Cav and Cav-BP) reduced after 40 min and converged at the end of the test. At this time, the temperature of the air in the cavity and, the temperature between the PCM mat and gypsum plasterboard were the same, which might be due to the melting of the poly film mat. Time taken to reach 100 °C was 17, 23, 27, 31 and 77 min for PB1-BP, BP-Cavity, Cavity-BP, BP-PB2 and PB2-AS, respectively.

Figure 22 (b) shows the individual thermocouple readings and the average temperature of the ambient side, measured on gypsum plasterboard (PB2). Average and maximum insulation failure temperatures of 165 and 205 °C were observed at 93 and 95 min (initial temperature was 25 °C) and the test was terminated at 116 min.

Figure 22 (c) shows the average time-temperature profiles of stud HF and CF. The maximum HF temperature was 710 °C at 116 min while the maximum difference between HF and CF temperatures was 110 °C at 45 min. The critical HF temperature of 400 °C for a load ratio of 0.5 [25] was reached at 51 min with the corresponding CF temperature of 290 °C. Hence a structural adequacy based fire resistance time of 51 min can be achieved.
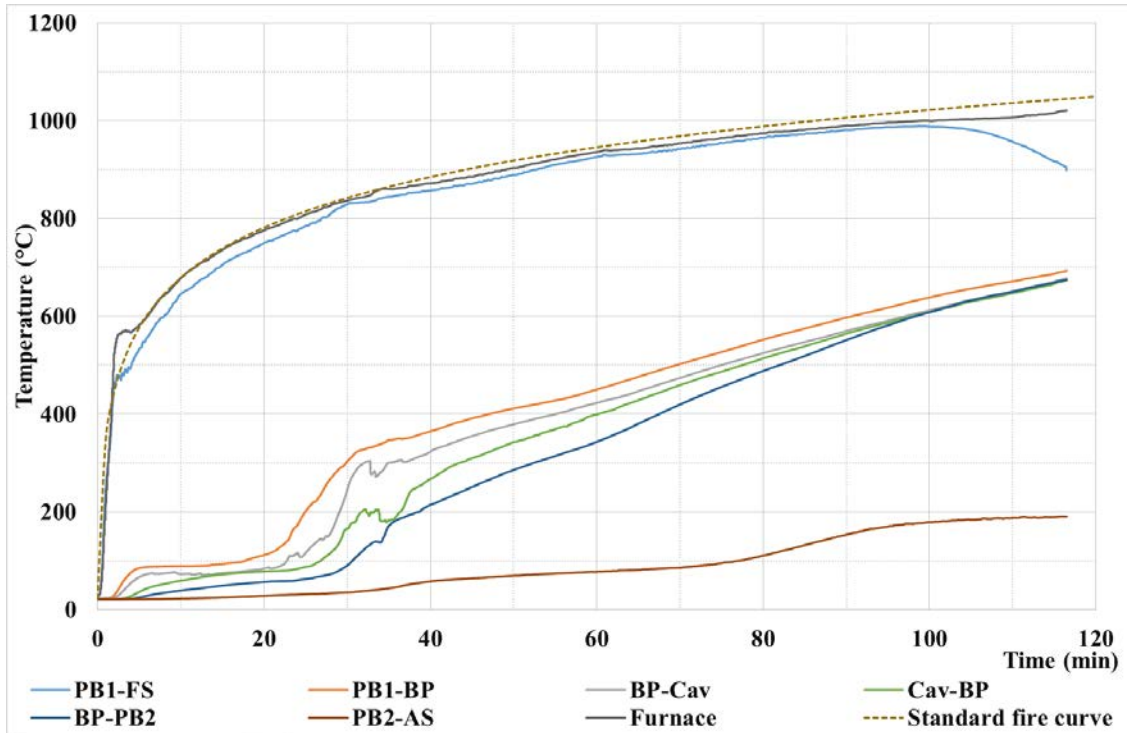
(a) Average gypsum plasterboard and bio-based PCM mat surface temperatures
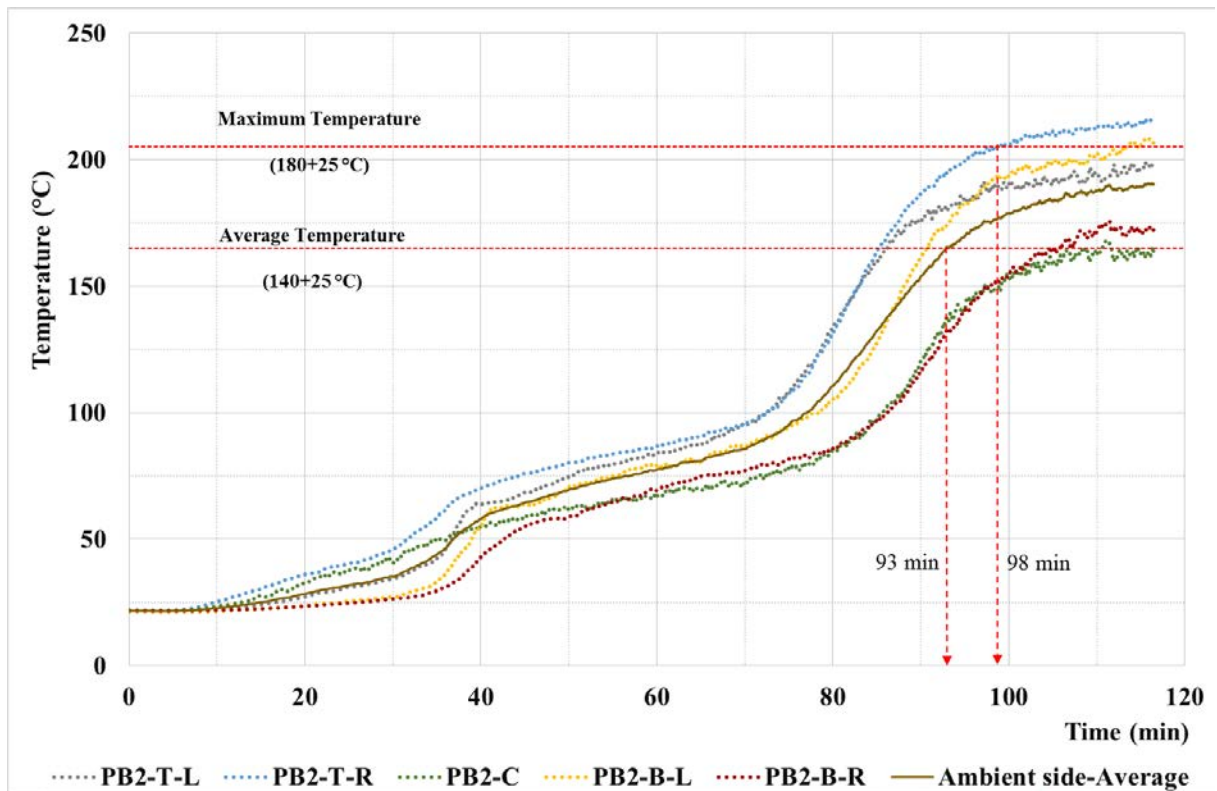
(b) Ambient side gypsum plasterboard (PB2) temperatures
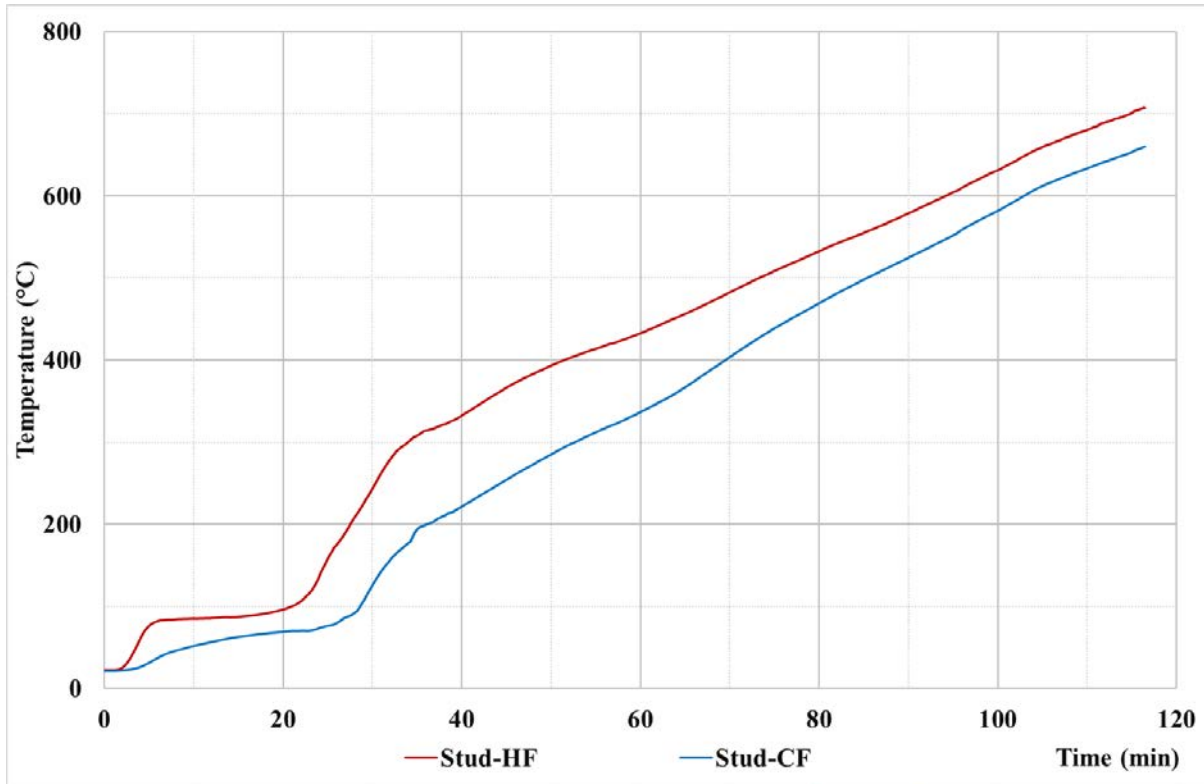
(c) Average stud HF and CF temperatures

Figure 22. Fire test results of Test specimen 5

Since the thicknesses of the boards tested were not the same, the ratio of insulation failure time to total board thickness was calculated from the insulation failure times obtained from the small-scale standard fire tests for comparison purposes. These ratios are 2.56, 1.22, 2.10 and 1.18 min/mm for gypsum plasterboard, fibre cement board, magnesium sulphate board and vermiculux board, respectively. They clearly show that the fire resistance times of vermiculux and fibre cement boards are much lower compared to the other two boards of the same thickness. Overall, gypsum plasterboard lined wall exhibited the best performance. These findings correlate well with the thermal property results in Section 3.

6. Discussions

Although an increased heat absorption capacity was observed for magnesium sulphate boards compared to gypsum plasterboards due to the additional specific heat peak observed at elevated temperatures, magnesium sulphate board exhibited higher values of mass loss and thermal conductivity than gypsum plasterboard. This higher mass loss will lead to severe cracking while its higher thermal conductivity will mean higher heat transfer in fire. Further, the variations in specific heat, mass loss and thermal conductivity of magnesium sulphate board

are similar to those observed for magnesium oxide boards at elevated temperatures. This shows that the behaviour of magnesium sulphate board in a fire will be similar to that of magnesium oxide boards, that is, when used in LSF wall systems it will lead to premature integrity failures due to severe cracking as observed for magnesium oxide board lined walls in [7].

During the standard fire tests of LSF walls (Section 4), different observations were seen for each type of wallboards. Among them, gypsum plasterboard lined wall performed well without any cracking at higher temperatures. On the other hand, fibre cement board, magnesium sulphate board and vermiculux board showed severe cracking at higher temperatures during the tests. However, the crack formation is completely different for each board. Fibre cement board had cracks through the vertical joints while magnesium sulphate board had cracks near the screw locations, which might be due to the restraint and higher mass loss. Cracks in vermiculux board formed in both vertical and horizontal directions, regardless of screw locations. This might be due to the expansion/swelling of vermiculite in the board, where the added vermiculite content is too high to compensate for the shrinkage caused during a fire.

The LSF wall lined with gypsum plasterboards outperformed walls lined with other wallboards with an insulation criterion based failure time of 82 min. The fibre cement board lined LSF wall gave the lowest insulation failure time of 22 min, whereas the insulation failure times of magnesium sulphate board and vermiculux board (42 and 47 min) are between those of the above two boards. The above findings are valid even after allowing for the difference in board thicknesses. Further, the structural adequacy based fire resistance times of LSF wall with a load ratio of 0.5 was estimated as 36, 16, 30 and 24 min for the LSF wall systems lined with gypsum plasterboard, fibre cement board, magnesium sulphate board and vermiculux board, respectively. Table 2 gives the failure times based on insulation and structural adequacy and the maximum hot flange temperatures for all the tested LSF walls. Overall, these results have shown the superior fire performance of gypsum plasterboard lined LSF walls. A higher hot flange temperature of 650 °C was observed in both gypsum plasterboard and vermiculux board lined LSF walls. However, the time taken to reach this temperature was higher for gypsum plasterboard lined LSF wall.

Table 2. Summary of fire test results

Test No	Description	Insulation failure time (min)		Structural failure time (min)	Max. stud temperature at the end (°C)	Test Duration (min)	Ratio* (min/mm)
		Avg	Max				
1	Gypsum plasterboard	82	103	36	650	140	2.56
2	Fibre cement board	22	25	16	530	27	1.22
3	Magnesium sulphate board	42	43	30	550	44	2.10
4	Vermiculux board	47	47	24	650	55	1.18
5	External gypsum plasterboard and bio-based PCM mat inside	93	95	51	710	116	-

Note: Ratio* = Insulation failure time / total board thickness (min/mm)

The use of bio-based PCM mats in the best performing LSF wall lined with gypsum plasterboards increased the fire resistance further by 11 min (from 82 to 93 min) based on the insulation failure criterion. Further, the structural adequacy based failure time was estimated as 51 min for a load ratio of 0.5, in comparison with 36 min. These results reveal that the bio-based PCM mat together with external gypsum plasterboard linings can be used to improve the thermal mass without reducing the fire resistance of LSF walls.

Paraffin PCM incorporated plasterboards (PCM-plasterboards) are also used in buildings to increase the thermal storage capacity. A recent study by Gnanachelvam et al. [16] based on small-scale fire tests of LSF walls showed that the fire resistance of wall systems could be affected by PCM-plasterboards' flammable behaviour. Insulation failure time was reduced by 77 min (from 233 to 156 min) when a combination of gypsum plasterboard and PCM-plasterboard was used instead of two layers of gypsum plasterboard [16]. The use of PCM-plasterboards on the exposed side increases the fire intensity due to the additional fuel they provide in fire. Although the PCM-plasterboard was placed behind a gypsum plasterboard layer within the LSF wall tested in this study, the fire performance was affected soon after the first

gypsum plasterboard layer started to fall-off. This will also lead to reductions in the structural adequacy of CFS studs [16]. However, the use of bio-based PCM mats with single layer gypsum plasterboard lined LSF wall increased its insulation based failure time by 11 min. This is due to their relatively high ignition resistance and significantly less flammability compared to paraffin-based PCMs. Therefore, incorporating the bio-based PCM mat in the LSF wall systems lined with two layers of gypsum plasterboards on both sides can increase the insulation based failure time to about 240 min, which is the maximum requirement in many cases according to the Australian building requirements [25]. Importantly, this gypsum plasterboard – bio-based PCM mat combination provides a solution to the LSF wall requirement of combined fire resistance and thermal performance.

7. Conclusions

This paper has presented the details of an experimental study on the fire resistance of LSF walls lined with different types of wallboards. Thermal property tests of selected wallboards and small-scale standard fire tests of non-load bearing LSF walls lined with gypsum plasterboard, fibre cement board, magnesium sulphate board and vermiculux board were conducted in this study. Small-scale standard fire test series also included a fire test of thermal mass improved LSF wall with gypsum plasterboard as the exterior lining and bio-based PCM mat as the interior lining. Thermal property test results showed that magnesium sulphate board has a very high mass loss of 43% at elevated temperatures, compared to 23% mass loss caused by dehydration in gypsum plasterboard. Its mass loss behaviour is very similar to that of magnesium oxide boards. Small-scale standard fire tests of LSF walls showed that the use of magnesium sulphate boards reduced the fire resistance of LSF walls with severe crack formation, as was observed for magnesium oxide boards in [7].

Standard fire tests showed that the failure of all the non-load bearing LSF walls lined with different wallboards was based on the average insulation failure criterion. The LSF wall lined with gypsum plasterboards performed significantly better than those lined with other wallboards. The fibre cement board lining provided the lowest fire resistance, whereas the fire resistance of magnesium sulphate board and vermiculux board falls between the other two boards. An insulation based fire resistance time of 82 min was achieved for gypsum board lining while about 45 min was achieved for the other boards except fibre cement board. The use of bio-based PCM mat together with external gypsum plasterboard lining increased the fire resistance time of LSF wall to 93 min. Although load bearing walls were not tested, the

measured time-temperature profiles of studs indicate that the structural adequacy based fire resistance time could also be increased. Further, the use of bio-PCM mats in LSF walls lined with two layers of plasterboards is likely to enhance the fire resistance times of LSF wall systems significantly. Overall, this study has shown that the use of bio-based PCM mat to improve the thermal mass of LSF walls with the best performing gypsum plasterboard lining provides higher fire resistance without increasing the fire risk, thus providing a solution to the LSF wall requirement of combined fire resistance and thermal performance.

Acknowledgements

References

[1]   Rokilan, M. and Mahendran, M., *Elevated temperature mechanical properties of cold-rolled steel sheets and cold-formed steel sections.* Journal of Constructional Steel Research, 2019. 105851.

[2]   Feng, M. and Wang, Y.C., *An experimental study of loaded full-scale cold-formed thin-walled steel structural panels under fire conditions.* Fire Safety Journal, 2005. 40(1): pp. 43-63.

[3]   Kodur, V.K.R. and Sultan, M.A., *Factors Influencing Fire Resistance of Load-bearing Steel Stud Walls.* Fire Technology, 2006. 42(1): pp. 5-26.

[4]   Nassif, A.Y., Yoshitake, I., and Allam, A., *Full-scale fire testing and numerical modelling of the transient thermo-mechanical behaviour of steel-stud gypsum board partition walls.* Construction and Building Materials, 2014. 59: pp. 51-61.

[5]   Ariyanayagam, A.D. and Mahendran, M., *Fire tests of non-load bearing light gauge steel frame walls lined with calcium silicate boards and gypsum plasterboards.* Thin-Walled Structures, 2017. 115: pp. 86-99.

[6]   Chen, W., Ye, J., Bai, Y., and Zhao, X.-L., *Improved fire resistant performance of load bearing cold-formed steel interior and exterior wall systems.* Thin-Walled Structures, 2013. 73: pp. 145-157.

[7]   Rusthi, M., Ariyanayagam, A., Mahendran, M., and Keerthan, P., *Fire tests of Magnesium Oxide board lined light gauge steel frame wall systems.* Fire Safety Journal, 2017. 90: pp. 15-27.

[8]   Wang, Y., Chuang, Y.-J., and Lin, C.-Y., *The Performance of Calcium Silicate Board Partition Fireproof Drywall Assembly with Junction Box under Fire.* Advances in Materials Science and Engineering, 2015. 2015: pp. 12.

[9]   Soares, N., *Thermal energy storage with phase change materials (PCMs) for the improvement of the energy performance of buildings.* 2015, University of Coimbra: Coimbra. pp. 216.

[10]   Asimakopoulou, E.K., Kolaitis, D.I., and Founti, M.A., *Fire safety aspects of PCM-enhanced gypsum plasterboards: An experimental and numerical investigation.* Fire Safety Journal, 2015. 72: pp. 50-58.

[11]   McLaggan, M.S., Hadden, R.M., and Gillie, M., *Flammability assessment of phase change material wall lining and insulation materials with different weight fractions.* Energy and Buildings, 2017. 153(Supplement C): pp. 439-447.

[12]   McLaggan, M.S., Hadden, R.M., and Gillie, M., *Fire Performance of Phase Change Material Enhanced Plasterboard.* Fire Technology, 2018. 54(1): pp. 117-134.

[13]   Kosny, J., Kossecka, E., Brzezinski, A., Tleoubaev, A., and Yarbrough, D., *Dynamic thermal performance analysis of fiber insulations containing bio-based phase change materials (PCMs).* Energy and Buildings, 2012. 52: pp. 122-131.

[14]   Sharma, A., Tyagi, V.V., Chen, C.R., and Buddhi, D., *Review on thermal energy storage with phase change materials and applications.* Renewable and Sustainable Energy Reviews, 2009. 13(2): pp. 318-345.

[15]   Ramakrishnan, S., Wang, X., Sanjayan, J., and Wilson, J., *Thermal performance of buildings integrated with phase change materials to reduce heat stress risks during extreme heatwave events.* Applied Energy, 2017. 194: pp. 410-421.

[16]   Gnanachelvam, S., Ariyanayagam, A., and Mahendran, M., *Fire resistance of light gauge steel framed wall systems lined with PCM-plasterboards.* Fire Safety Journal, 2019. 108: pp. 102838.

[17]   Martins, J.A., Gomes, C.M., Fontanini, P., and Dornelles, K., *Comparative analysis on thermal performance of MgO and fiber cement boards applied to light steel frame building systems.* Journal of Building Engineering, 2019. 21: pp. 312-316.

[18]   Jays, N., Olofinjana, A., and Young, D.J., *Assessing variability in the hygrothermal performance of magnesium oxide (MgO) cladding products of the Australian market.* Construction and Building Materials, 2019. 203: pp. 491-500.

[19]   McArthur, H. and Spalding, D., *Engineering Materials Science Properties, Uses, Degradation and Remediation.* 2004: Horwood publishing limited. 577.

[20]   ASTM E1269-11, *Standard Test Method for Determining Specific Heat Capacity by Differential Scanning Calorimetry,* West Conshohocken, USA, 2011

[21]   ASTM E1461-13, *Standard Test Method for Thermal Diffusivity by the Flash Method,* West Conshohocken, PA 19428-2959. USA, 2013

[22]   Gomes, C. and Camarini, G., *Magnesium Oxysulfate Fibercement.* Vol. 600. 2014. 308-318.

[23]   Standards Australia, *Method for fire test on building materials, components and structures, Part-4: Fire-resistance test of elements of construction*, Sydney, Australia, 2014

[24]   Gunalan, S. and Mahendran, M., *Fire performance of cold-formed steel wall panels and prediction of their fire resistance rating.* Fire Safety Journal, 2014. 64: pp. 61-80.

[25]   Australian Building Codes Board, *National Construction Code,* Canberra, Australia, 2019